1.0

4.5
5.0
5.6
6.3

2.8 2.5

3.2 2.2

3.6

4.0

1.1

2.0

1.8

1.25 1.4 1.6

MICROCOPY RESOLUTION TEST CHART
NATIONAL BUREAU OF STANDARDS-1963-A

NRL Memorandum Report 3732

The Physics and the Chemistry of NRL Master Code for the Disturbed E and F Regions

A. W. ALI

Plasma Physics Division

(12)

March 1978

D D C

RECEIVED
APR 27 1978
B

NAVAL RESEARCH LABORATORY
Washington, D.C.

NRL-M-3732

REPORT DOCUMENTATION PAGE	READ INSTRUCTIONS BEFORE COMPLETING FORM

1. REPORT NUMBER	2. GOVT ACCESSION NO.	3. RECIPIENT'S CATALOG NUMBER
NRL Memorandum Report 3732		Memorandum rept.,

4. TITLE (and Subtitle)	5. TYPE OF REPORT & PERIOD COVERED
THE PHYSICS AND THE CHEMISTRY OF NRL MASTER CODE FOR THE DISTURBED E AND F REGIONS.	Interim report on a continuing NRL problem.
	6. PERFORMING ORG. REPORT NUMBER

7. AUTHOR(s)	8. CONTRACT OR GRANT NUMBER(s)
A. W. Ali	S99QAXH D411 54 p.

9. PERFORMING ORGANIZATION NAME AND ADDRESS	10. PROGRAM ELEMENT, PROJECT, TASK AREA & WORK UNIT NUMBERS
Naval Research Laboratory Washington, D. C. 20375	NRL Problem H02-27D Project HD 0 1043

11. CONTROLLING OFFICE NAME AND ADDRESS	12. REPORT DATE
Defense Nuclear Agency Washington, D.C. 20305	Mar 78
	13. NUMBER OF PAGES
	68

14. MONITORING AGENCY NAME & ADDRESS(If different from Controlling Office)	15. SECURITY CLASS. (of this report)
	UNCLASSIFIED
	15a. DECLASSIFICATION/DOWNGRADING SCHEDULE

16. DISTRIBUTION STATEMENT (of this Report)

Approved for public release; distribution unlimited.

17. DISTRIBUTION STATEMENT (of the abstract entered in Block 20, If different from Report)

18. SUPPLEMENTARY NOTES

This work was performed at the Naval Research Laboratory under the auspices of the Defense Nuclear Agency under subtask S99QAXHD411, work unit code 15 and work unit title Reaction Rates Essential to Propagation.

19. KEY WORDS (Continue on reverse side if necessary and identify by block number)

E and F Regions
Disturbed ionosphere
Deionization
Reaction rates

20. ABSTRACT (Continue on reverse side if necessary and identify by block number)

The detailed Physics and the Chemistry of NRL Master Code for the Deionization Phase of the Disturbed E and F Regions are presented. Important physical processes are delineated and the current reaction rates, incorporated in the Code, are given.

DD FORM 1473 EDITION OF 1 NOV 65 IS OBSOLETE
1 JAN 73
S/N 0102-014-6601

i

251 950

CONTENTS

iii

I INTRODUCTION

The E and F regions of the ionosphere can be ionized (thus disturbed) under a variety of natural and man-made disturbing agents. Among these are: sun flares, energetic particle precipitations (which causes auroras), high power radars, high energy electron beams and nuclear bursts. The degree of the ionization, the spatial extent of the disturbed ionosphere and its relaxation time, depend clearly on the extent of the energy deposited. Such a disturbed atmosphere will have measurable and damaging effects on the communication and detection systems. Therefore, a complete understanding of the disturbed E and F regions is essential. This understanding will help to assess the impact of the disturbance on the communication and detection systems.

The disturbance in the E and F regions, due to a nuclear effect, e.g., can be summed up as to constitute the ionization of the medium and its subsequent motion accompanied by the deionization and the ultimate relaxation to the ambient condition of the atmosphere. The ionization and the deionization processes play a very important role in the complete analysis of the disturbed atmosphere. This report deals primarily with this aspect of the problem.

The disturbed atmosphere contains atomic and molecular ions, free electrons, neutrals and a host of excited species. A large number of atomic, molecular and chemical processes occur in such an ionized medium. The ionization and the deionization processes are accompanied by a wide range of emission in the ultraviolet, visible and infrared. Therefore, the disturbed atmosphere produces two very important agents that impact on the communication and detection systems. These are: the free electrons and the emitted radiation. To assess the impact of these, a detailed analysis of

the disturbed atmosphere is required. This entails a time dependent physical model which is complete in its description of the phenomena. The approach, generally, has been to describe the phenomena by a set of rate equations which predict the time histories of all appropriate species and relevant kinetic temperatures. This approach has led to the development of multi-species codes whose complexities depend on the number of species, reactions and temperatures that enter into the code.

The NRL Master Code is such a multispecies code. From its first inception as a disturbed F region deionization code[1], evolved to include ionization due to incoming radiation[2], describe[3] the disturbed E region, and provide volume emission over a wide range of visible and infrared radiation. It was used to obtain simpler deionization codes to be utilized in conjunction with large scale MHD codes. The Simple Code[3], with emphasis on electron density, generally, has predicted[4] electron densities within 20% of the Master Code.

One of the important characteristics of a multispecies code is to re-main dynamic and to incorporate the most appropriate and up-to-date reaction rates available. In this report we describe the current NRL Master Code and give the current reaction rates it incorporates. We discuss in detail the physics and the chemistry of the disturbed E and F regions, point out important processes that provide an overall view of the relaxation phenomenon.

II DISTURBED E AND F REGIONS CONSTITUENTS

The major neutral species in the ambient E and F regions are N_2, O_2 and O, where the peak densities are $\sim 10^{11}$ cm^{-3}. This region, however, is weakly ionized, due to the ionizing radiation from the sun, with a peak electron density of $\sim 5 \times 10^5$ cm^{-3}. For all practical purposes, one may ignore this ionization level when the E and F regions are subject to high intensity radiation from nuclear weapons effects. Thus, one can consider the region to be made of the above neutrals only.

When the E and F regions are subjected to an intense ionizing force, one may consider the analysis of the problem in two phases. The first phase coincides with the duration of the ionizing force and may be termed as the deposition phase. This phase is dominated by ionization of the medium and the occurance of a large number of processes which are physical and chemical in nature. The second phase starts with the termination of the ionizing force and is generally called the deionization phase. During this phase, fractional ionization may occur, however, it may not be as important in comparison with the major trend of the relaxation which is accompanied by a large number of atomic and chemical processes.

A The Deposition Phase

The incident radiation consisting of X-ray and UV spectral lines will dissociate O_2 and ionize N_2, O_2 and O resulting in N_2^+, O_2^+, O^+ and free electrons. Dissociation of O_2 leads to the formation of oxygen atoms in the ground, and exicted $O(^1D)$, states. The dissociative recombinations of N_2^+ and O_2^+ produce N, $N(^2D)$, O, $O(^1D)$ and $O(^1S)$. However, the collisions of the free electrons with atomic and molecular species adds $N(^2P)$, $N_2(A^3\Sigma)$, $O_2(a^1\Delta)$ and $O_2(b^1\Sigma)$, while chemical reactions e.g. that of $N(^2D)$ with O_2 forms NO. These neutral metastable species and NO are subsequently ionized

under the influence of the continuing radiation, producing N^+, $N^+(^1D)$, $N^+(^1S)$, 0^+, $0^+(^2D)$, $0^+(^2P)$ and $N0^+$. The population densities of these metastable ions are affected by collisions with the free electrons as well. Thus, the constituents of the disturbed E and F regions are: electrons and neutral and ionized species which are in their ground and excited metastable states and are atomic or molecular in nature. These species, which are in the NRL Master Code, are given in Table I with their excitation energies, lifetimes and the radiation they emit.

TABLE I

Species	Excitation Energy (eV)	Life-Time (sec)	Emission	Ref.
$N_2(X^1\Sigma)$	-	-	-	-
$N_2(A^3\Sigma)$	6.1	1.3, $\Sigma = 0$ 2.7, $\Sigma = 1, -1$	UV band	5,6,7
$N_2^+(X^2\Sigma)$	-	-	-	-
$O_2(X^3\Sigma)$	-	-	-	-
$O_2(a^1\Delta)$	1.00	3.9×10^3	1.27 μ	5,7,8
$O_2(b^1\Sigma)$	1.60	12.0	Visible	5,7,9
$O_2^+(X^2\pi)$	-	-	-	-
$O_2^+(a^4\pi)$	4.0	Long	Visible	5,10
$NO(X^2\pi)$	0.23,V=1 0.46,V=2	~ msec	5.4 μ 2.7 μ	-
$NO^+(X^1\Sigma)$	0.29,V=1 0.58,V=2	~ msec	4.28 μ 2.14 μ	-
$N(^4S)$	-	-	-	-
$N(^2D)$	2.37	2×10^5	5,200 Å	11
$N(^2P)$	3.57	13.0	10,400 Å	11
$N^+(^3P)$	-	-	-	-
$N^+(^1D)$	1.89	250.0	6,548 Å 6,584 Å	11
$N^+(^1S)$	4.05	0.92	5,755 Å	11
$O(^3P)$	-	-	-	-
$O(^1D)$	1.96	150	6,300 Å 6,363 Å	11
$O(^1S)$	4.18	0.74	5,577 Å	11
$O^+(^4S)$	-	-	-	-
$O^+(^2D)$	3.32	10^4	3,728 Å	11
$O^+(^2P)$	5.01	5.84	7,320 Å 7,330 Å	11

However, in addition to the metastable states presented in Table I, several shortlived (μ sec) excited states also arise. These states (given in Table II) arise due to the fact that N_2 and O_2 have several distinct ionization continuua with different ionization thresholds. They subsequently decay to the ground state of the ion with characteristic emissions of their own. These and other optically allowed states, however, arise by electron impact collisions with the ion ground states as well.

TABLE II

Species	Excitation Energy (eV)	Life-Time (sec)	Emission	Ref.
$N_2^+(A^2\pi)$	1.12	13.9 μsec, $v' = 1$	IR band	5,7,12
		7.3 μsec, $v' = 8$		
$N_2^+(B^2\Sigma)$	3.17	59 nsec, $v' = 0$	UV band, visible	5,7,13
$O_2^+(A^2\pi)$	4.8	μsec	Visible band	5,7,14

The analysis of the species and their time histories during the deposition phase, assuming one knows the magnitude of the incident ionizing flux at each spectral line, requires reliable photo-absorption, and photo-ionization cross sections of the elements of the region. These are required for each photon energy. Of more importance, however, is the partial photo-ionization cross sections for each state. This provides information on the initial energy distribution of the photo-electrons and the density distribution of the metastable states. A detailed analysis of the deposition phase will be the subject of a forthcoming report.

During this phase, the disturbed atmosphere is characterized by three temperatures, which control the distribution of the species. These tempera-

tures are: the electron temperature, T_e, the heavy particle (atoms, molecules and their ions) temperature, T_a, and the N_2 vibrational temperature T_v. These temperatures continue to develop after the deposition phase and control the course of the deionization and emission. However, it should be pointed out that during this phase the electrons are heated by the photoelectrons and that this heating term is terminated with the end of the incident radiation. Apart from this heating source, the processes which control the electron temperature, are the same as those during the deionization phase.

B Deionization Phase

The termination of the incident radiation will start a new phase in the disturbed atmosphere, whereupon the ionized region will start to relax to its ambient condition. The initial conditions for this deionization phase are determined by the duration of the radiation, its intensity and the elementary processes (physical and chemical reactions) which take place.

The constituents of the disturbed E and F regions at the start of the deionization phase are given in Table I. The species of this table and three characteristic temperatures evolve in time describing the relaxation of the disturbed atmosphere.

-7-

## III THE DEIONIZATION OF THE DISTURBED E AND F REGIONS

The disturbed ionosphere tends to relax once the ionizing force is terminated. The relaxation towards the ambient condition is accomplished by a large number of reactions, some are direct and others are indirect. These reactions differ from each other in magnitude and their dependence on a particular temperature. Some depend on the electron temperature, while others depend on vibrational or kinetic temperatures. However, a general picture of the deionization processes can be drawn in which several distinct and well understood reactions play the dominant role.

The constituents of the disturbed E and F regions are illustrated in Table I. These species, apart from the free electrons, can be divided into three groups which are: molecular ions, atomic ions, and neutrals. The species in each group, however, can be in ground, excited or both states and they all play a role in the deionization.

The processes which remove the electrons are the dissociative recombinations

$$N_2^+ + e \rightarrow N^* + N \tag{1}$$

$$O_2^+ + e \rightarrow O + O^* \tag{2}$$

$$NO^+ + e \rightarrow N^* + O \tag{3}$$
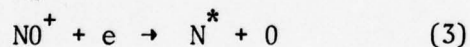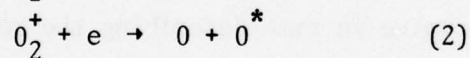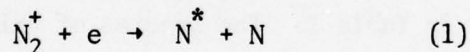
and the radiative recombinations

$$N^+ + e \rightarrow N + h\nu \tag{4}$$

$$O^+ + e \rightarrow O + h\nu \tag{5}$$
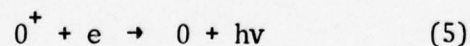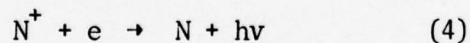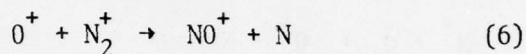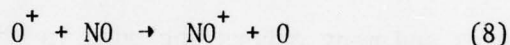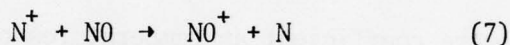
These two processes depend on the electron temperature, and have very different recombination rate coefficients. At room temperature, the dissociative recombination[15] rate coefficients are $\sim 10^{-7}$ cm^{-3}/sec compared to $\sim 10^{-12}$ cm^3/sec for the radiative recombination[16]. Clearly

the dissociative recombination is an efficient way to remove the electrons whenever the molecular ion densities are large enough. The two dissociative recombinations (1) and (2) proceed immediately because of the abundance of the nitrogen and oxygen molecules. However, the removal of the electrons by the dissociative recombination of NO^+ has to await the formation of this ion whose neutral parents are not abundant in the ambient ionosphere. This ion (NO^+) is formed, however, through the following reaction

$$O^+ + N_2^+ \rightarrow NO^+ + N \tag{6}$$

where it depends on the vibrational[17] temperature of N_2 as well as the ion kinetic temperature[18]. Other indirect paths for the formation of NO^+ are the charge exchange processes

$$N^+ + NO \rightarrow NO^+ + N \tag{7}$$

$$O^+ + NO \rightarrow NO^+ + O \tag{8}$$

These two processes depend on NO whose density, generally, builds up in the disturbed atmosphere through the following reactions:

$$N(^2D) + O_2 \rightarrow NO + O \tag{9}$$

$$O + N_2 \rightarrow NO + N \tag{10}$$

$$N + O_2 \rightarrow NO + O \tag{11}$$
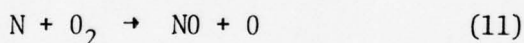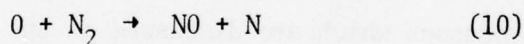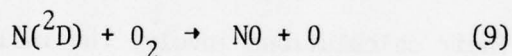
Reactions 9-11 depend on the kinetic temperature of the neutral atom and the higher the temperature the faster is the rate for the formation of NO.

The processes 6-8 are reactions that convert an atomic ion into a molecular ion which in turn dissociatively recombines with the free electron at a fast rate. This conversion, therefore, is very important because it speeds up the removal of the electron. There are several other processes similar to reactions 7 and 8 which convert an atomic ion into a molecular ion. These are:

$$O^+(^2D) + N_2 \rightarrow N_2^+ + O \qquad (12)$$

$$O^+ + O_2 \rightarrow O_2^+ + O \qquad (13)$$

$$N^+ + O_2 \rightarrow O_2^+ + N \qquad (14)$$
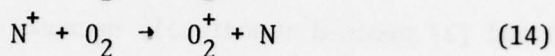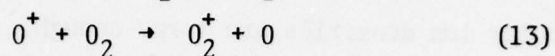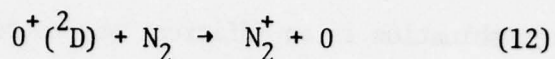
These reactions 1-14 present important processes which lead towards the deionization of the disturbed atmosphere. However, there are clearly many intermediate reactions which occur that affect the deionization as well. We give an example of such a reaction,

$$N^+ + O \rightarrow O^+ + N \qquad (15)$$

which enhances the formation of NO^+ via reaction (6). The importance of (15) is obvious, whenever the density of O_2 is very low. However, the above reaction, (15), does not have a measured or a reliable theoretical estimate for its rate coefficient at temperatures of interest.

These processes and many others included in the NRL Master Code[3] depend, as we indicated earlier, on the electron temperature, the N_2 vibrational temperature and the heavy particle temperature which have to be calculated. Their calculations involve the inclusion of a large number of elementary processes which are discussed in the next sections.

IV DISTURBED E AND F REGIONS REACTIONS

In Section III, we presented several reactions which play an important role in the deionization. However, in reality, a large number of reactions occur in the course of the deionization. These reactions control the time behavior of the individual species, their emissions, the three temperatures, T_e, T_v and T_a as well as the deionization itself, directly or indirectly. Therefore, it is essential that these processes be delineated and their respective rate coefficients known with a good degree of reliability. In this section we present these reactions and their rate coefficients.

A Dissociative and Radiative Recombinations

The dissociative recombination rate coefficients of N_2^+, O_2^+ and NO^+ have been measured. These rates depend on the electron temperature[15] as well as the molecular ion vibrational temperature[19,20]. However, the measurements are invariably carried out as a function of the electron temperature with very little or no variation of the vibrational temperature. For the recombination of N_2^+ and O_2^+, the electron temperature was varied[21] from 300 to 5000°k. Expressions fit to this data for the rate coefficients are given in Table III. Recent measurements[22] of O_2^+ recombination agree very well with the previous measurements of Biondi and his colleagues[21]. However, the recombination of NO^+, currently, have two very different temperature dependent rates. The rate coefficient measured by Huang et al[23] has a temperature dependence of $T_e^{-0.37}$ compared to the measurement of Walls & Dunn[22] with a $T_e^{-0.83}$ variation. This should be compared with a temperature dependence of $T_e^{-1.2}$ compiled by Biondi[24] from several measurements[25-27], which was utilized previously in the NRL Master Code[3]. The two current[22,23] rate coefficients for NO^+ recombination are given in Table III where a fit was obtained from the experimental data[22,23]. A

-11-

comparison of these three rate coefficients for NO^+ is shown graphically in Fig. 1. From this figure, it is seen that the rate coefficient of Huang, et al[23] is large compared to that of Walls and Dunn[22], even though the last measurement is undoubtly for NO^+ being in its ground vibrational state (V=0). The total rate coefficient with its dependence on both the electron and the vibrational temperature should follow[19]

$$D \sim T_e^{-\frac{1}{2}} (1 - e^{-h\nu/T_v})$$

which makes the two rates[22,23] somewhat of a puzzle at this juncture and clearly requires further measurements.

TABLE III

Dissociative Recombinations

Symbol	Reaction	Rate Coefficient	Reference
D_1	$N_2^+ + e \rightarrow N + N'$	$4.3 \times 10^{-8} (T_e)^{-0.39}$	21
D_2	$NO^+ + e \rightarrow N' + 0$	(a) $9.8 \times 10^{-8} (T_e)^{-0.37}$	23
		(b) $2.0 \times 10^{-8} (T_e)^{-0.83}$	22
D_3	$0_2^+ + e \rightarrow 0' + 0$	$1.5 \times 10^{-8} (T_e)^{-0.7}, T_e \leq 0.1 eV$	21
		$2.1 \times 10^{-8} (T_e)^{-0.5}, T_e > 0.1 eV$	

In addition to the magnitude and temperature dependence of these dissociative recombinations, the branching ratios of the products of these reactions are required. In the disturbed atmosphere, the importance of the branching ratios are very obvious. They influence emission, the electron and heavy particle temperatures and ultimately the deionization itself. A sensitivity study[28] of the effects of these branching ratios on the deionization of the disturbed F region were carried out previously to indicate their importance. Figure 2 shows the electron density for several sets of assumptions of the dissociative recombination products where at least a factor of three in the electron density can be seen at late times. Recent calculations
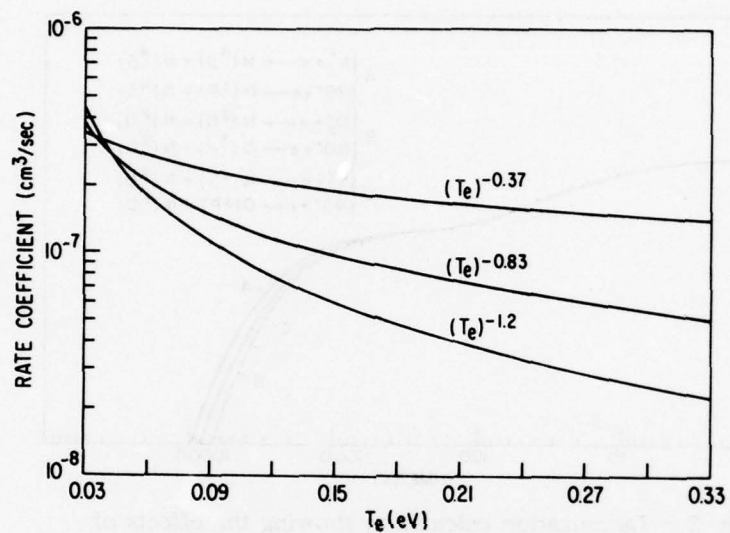
Fig. 1 — The dissociative recombination rate coefficients of NO$^+$ as a function of the electron temperature. (See text for details.)
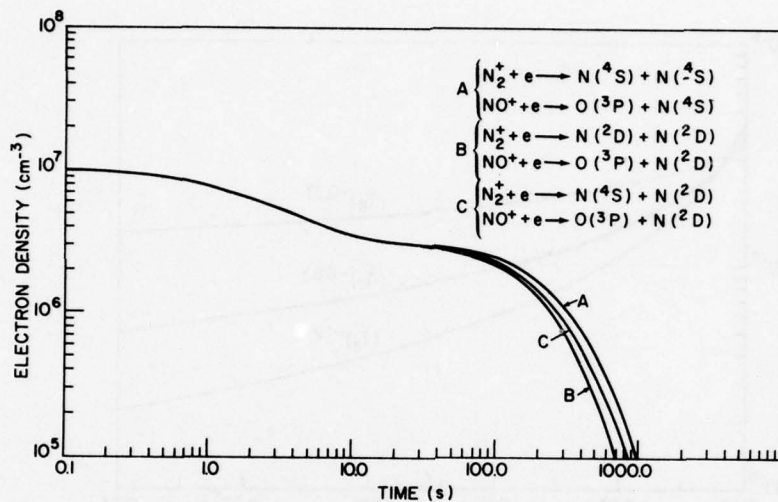
Fig. 2 — Deionization calculation showing the effects of
recombination products on the electron density.

by Michels[29] show that the products of the NO^+ dissociative recombination are ~ 100% $N(^2D)$ and 100% $O(^3p)$. More recently, however, Kley, et al[30], have indicated that the actual yield of $N(^2D)$ is ~ 76%. The dissociative recombination[31] of N_2^+, on the other hand, yields $N(^2D)$ and $N(^4S)$ with equal probability. However, the dissociative recombination[32] of O_2^+ yields 100% $O(^3p)$, 90% $O(^1D)$ and 10% $O(^1S)$.

The radiative recombination (Eq. 4 and 5) can be approximated by hydrogenic relations[16] with the following expression for the N^+ and O^+ recombination rate coefficients

$$\alpha = 3.9 \times 10^{-14} \sqrt{\frac{14}{T_e}} \left\{ 0.43 + \frac{1}{2} \log \frac{14}{T_e} \right\} \quad (16)$$

B Electron Impact Excitations and Deexcitations

During the deposition and the deionization phases of the disturbed atmosphere, the electrons undergo a large number of inelastic and super-elastic collisions. These collisions not only determine the electron temperature, but also control the distributions of a large number of species, thereby affecting the course of the deionization process. Therefore, these collision processes have to be identified and their respective rate coefficients obtained. Among these are; excitations and the deexcitations of the metastable species, the excitations of the optically allowed transitions of the electronic states of the species, the vibrational excitations and deexcitations of N_2 and O_2, electron ion collisions and ionization collisions.

In this section, the excitations of the species by low energy electrons (E < 5 eV) will be discussed and their rate coefficients will be given. The excitation rate coefficients are obtained from the relevant cross sections averaged with the electron velocity over a Maxwellian electron velocity distribution. In certain cases some of the rates are obtained from their respective collision strengths. For each excitation process,

-15-

the deexcitation rate coefficient can be obtained through the principle of the detailed balance.

B1 Inelastic Electron Collisions in N_2 and N_2^+

The nitrogen molecule constitutes a large energy sink to which the free electrons lose their energies. Among these sinks are the excitations of the ground state vibrational levels, the excitations of the electronic states and the ionization of the molecule . For low energy electrons the vibrational excitations become very important[33] in comparison with the rest of the processes.

B1.1 The Vibrational Excitations

The cross sections for the ground state vibrational levels up to $v=8$ have been measured[34,35] and several theoretical calculations exist[36,37,38]. One of these calculations[38], reproduces the experimental results very satisfactorily[39]. Using the measured cross sections[34], the excitation rate coefficients for eight ground state vibrational levels have been obtained[40]. These rate coefficients are shown in Fig. 3 and are tabulated in Table IV.

B1.2 The Electronic Excitations of N_2

The nitrogen molecule possesses a series of triplet electronic states, $A^3\Sigma$, $B^3\pi_g$, $C^3\pi_u$, etc. which are excited from the ground state of the molecule. Their excitations result in cooling the electrons and in the emission of well known bands. These bands are; the Vegard-Kaplan band $(A^3\Sigma \rightarrow X^1\Sigma)$ which is in the uv and the blue region of the Spectrum, the first positive band $(B^3\pi \rightarrow A^3\Sigma)$ which is in the visible and short wave infrared, and the second positive band $(C^3\pi \rightarrow B^3\pi)$ which is in the visible and the ultraviolet. These triplet states are short lived except for $A^3\Sigma$ which is metastable with a life-time[41] of 1 sec. Therefore, cascade from higher triplet states will further populate $A^3\Sigma$ state. The significance

-16-
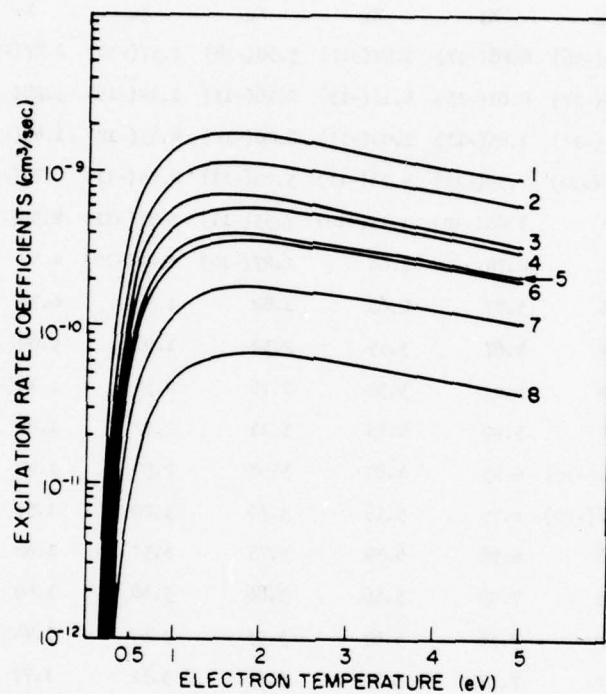
Fig. 3 — Excitation rate coefficients as a function of electron temperature for eight ground-state vibrational levels of N_2

N_2-Vibrational Excitation Rate Coefficients

T_e/x_v	x_1	x_2	x_3	x_4	x_5	x_6	x_7	x_8
0.1	1.98(-14)*	1.49(-16)	6.29(-17)	1.57(-17)	5.58(-18)	1.37(-18)	2.27(-19)	2.51(-20)
0.2	4.01(-12)	1.48(-12)	8.81(-13)	4.16(-13)	2.16(-13)	1.14(-13)	3.28(-14)	7.81(-15)
0.3	5.63(-11)	2.82(-11)	1.83(-11)	1.05(-11)	6.20(-12)	4.13(-12)	1.45(-12)	4.31(-13)
0.4	2.08(-10)	1.14(-10)	7.59(-11)	4.76(-11)	3.02(-11)	2.24(-11)	0.71(-12)	2.85(-12)
0.5	4.38(-10)	2.52	1.68(-10)	1.11(-10)	7.33(-11)	5.77(-11)	2.39(-11)	8.26(-12)
0.6	6.96(-10)	4.11	2.74	1.88	1.27(-10)	1.04(-10)	4.47	1.60(-11)
0.7	9.43(-10)	5.66	3.77	2.65	1.82	1.52	6.76	2.47
0.8	1.16(-9)	7.04	4.67	3.35	2.32	1.98	9.00(-11)	3.33
0.9	1.34	8.20	5.41	3.96	2.75	2.38	1.10(-10)	4.12
1.0	1.48	9.12	5.99	4.45	3.11	2.72	1.27	4.80
1.1	1.58	9.84(-10)	6.43	4.85	3.38	2.99	1.42	5.37
1.2	1.66	1.04(-9)	6.75	5.15	3.60	3.20	1.53	5.83
1.3	1.71	1.08	6.96	5.39	3.75	3.37	1.62	6.19
1.4	1.74	1.10	7.09	5.56	3.86	3.48	1.69	6.46
1.5	1.76	1.12	7.16	5.67	3.93	3.57	1.74	6.65
1.6	1.77	1.12	7.17	5.75	3.96	3.62	1.77	6.78
1.7	1.76	1.12	7.15	5.79	3.97	3.65	1.79	6.86
1.8	1.75	1.12	7.09	5.81	3.96	3.66	1.80	6.89
1.9	1.73	1.11	7.00	5.80	3.94	3.65	1.80	6.89
2.5	1.56	1.02(-9)	6.26	5.51	3.61	3.45	1.71	6.46
3.0	1.39	9.21(-10)	5.57	5.15	3.36	3.20	1.58	5.88
3.5	1.24	8.29	4.93	4.77	2.93	2.95	1.44	5.29
4.0	1.11(-9)	7.47	4.38	4.43	2.64	2.73	1.32	4.74
4.5	9.95(-10)	6.74	3.90	4.12	2.38	2.55	1.21	4.24
5.0	8.96(-10)	6.11(-10)	3.49(-10)	3.84(-10)	2.16(-10)	2.39(-10)	1.12(-10)	3.80(-11)

*Numbers in parenthesis indicate powers of 10 by which the entries are to be multiplied. Where no parenthesis are given the entries are multiplied by the power of 10 for the preceding entries.

of this state is that it contributes to the formation of $O(^1S)$ via

$$N_2(A^3\Sigma) + O(^3p) \rightarrow N_2(X^1\Sigma) + O(^1S) \qquad (17)$$
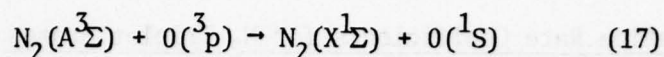
with a rate coefficient[42] of 3×10^{-12} cm^3 sec^{-1}. Furthermore, the $A^3\Sigma$ state is quenched by atomic oxygen and nitrogen[43]. This quenching (with a rate coefficient of $\sim 5 \times 10^{-11}$ cm^{-3}) will add to the thermal energy of the heavy particles.

The electron impact excitation cross sections for the triplet states have been calculated[44,45]. Measured cross sections exist for $A^3\Sigma$ (Ref. 46 and 47), $B^3\pi$ (Ref. 46 and 49), $C^3\pi$ (Ref. 46,49,50,51) and $D^3\Sigma$ (Ref. 52 and 53). However, the shapes and the peak values of these cross sections, whether experimental or theortical, are not in good agreement with each other[54]. A case in point is made in Table V showing the peak cross values for $A^3\Sigma$ state.

TABLE V

Peak Cross Section Values of $A^3\Sigma$

Magnitude $(10^{-17} cm^2)$	Ref.
5.25	47
3.00	46
12.00	45
15.00	44

The rate coefficients for the excitation of the triplet states, given in Table VI, are obtained using the calculated[44] cross sections, whose peaks were adjusted to the mean experimental values. For example, Cartwright's[44] calculated value for $A^3\Sigma$ state was divided by four to conform with the mean experimental value (see Table V).

-19-

TABLE VI

Electron Impact Excitation Rate Coefficients for N_2 Triplet States

T_e	$A^3\Sigma$	$B^3\Sigma$	$C^3\Sigma$	$D^3\Sigma$	$E^3\Sigma$
0.2	1.3(-23)	2.8(-25)	4.7(-33)	5.0(-38)	2.0(-35)
0.3	1.3(-18)	6.8(-20)	8.0(-25)	1.0(-28)	1.1(-26)
0.5	1.5(-14)	1.5(-15)	3.2(-18)	2.9(-21)	1.1(-22)
0.7	8.3(-13)	1.2(-13)	2.3(-15)	4.5(-18)	1.0(-16)
1.0	1.8(-11)	3.4(-12)	2.8(-13)	1.1(-15)	1.7(-14)
1.2	5.9(-11)	1.3(-11)	1.9(-12)	9.7(-15)	1.3(-13)
1.5	2.0(-10)	4.9(-11)	1.2(-11)	8.1(-14)	9.0(-13)
2.0	4.3(-10)	1.9(-10)	7.8(-11)	6.7(-13)	6.2(-12)
3.0	2.1(-9)	7.8(-10)	4.8(-10)	5.4(-12)	4.0(-11)
5.0	4.8(-9)	2.4(-9)	1.9(-9)	2.6(-10)	1.5(-10)

In addition to the triplet states discussed earlier, the nitrogen molecule has a large number of singlet states e.g.-$a^1\pi_g$, $c'^1\Sigma_u^+$, $a''^1\Sigma_g$, $w^1\Delta_g$, $b'^1\Sigma_u$, $b^1\pi$, etc. The excitation of $a^1\pi$ resulting in the Lyman-Birge-Hopfield band ($a^1\pi_g \rightarrow X^1\Sigma$) emission, which is in the ultraviolet, has received some theortical[45] and considerable experimental attention[46,47,55-58]. The most recent measurement[58] agrees very well with those of Borst[47] from threshold up to incident electron energy of 40 eV, and is slightly lower ~ 30% from measured values of Brinkmann and Trijmar[46]. This last cross section was utilized to obtain the excitation rate coefficient for $a^1\pi$ given in Table VII. As for the rest of the singlet states, calculations[45] exist only for $a''^1\Sigma$, $c'\Sigma$ and $b^1\pi$. However, measured cross sections exist[46] for some optically allowed transitions and singlet states grouped together. These cross sections[46] are utilized to give the rate coefficients for the optically allowed transitions and are given in Table VII.

TABLE VII

Rate coefficients for Electron Impact Excitations of $a^1\pi$, two optically allowed transitions with threshold energies of 12-13eV in N_2, also ionization of N_2 and excitation of $N_2^+(B)$.

T_e	$a(^1\pi)$	Opt. Group 2 & 4	N_2(Ioniz)	$N_2^+(B)$
0.1				3.3×10^{-21}
0.2	7.0(-31)		1.9(-43)	1.6(-14)
0.3	1.6(-23)		6.1(-32)	2.4(-12)
0.5	1.3(-17)	3.2(-20) 8.0(-21)	1.1(-22)	1.2(-10)
0.7	5.0(-15)	4.4(-17) 1.1(-17)	1.0(-18)	7.2(-10)
1.0	2.5(-13)	1.0(-14) 2.5(-15)	1.2(-15)	2.0(-9)
1.2	2.4(-12)	3.9(-13) 1.0(-13)	1.8(-14)	3.2(-9)
1.5	1.4(-11)	8.4(-13) 2.1(-13)	2.9(-13)	5.2(-9)
2.0	9.9(-11)	8.0(-12) 2.0(-12)	4.8(-12)	8.3(-9)
3.0	4.6(-10)	8.4(-11) 2.1(-11)	9.0(-11)	1.2(- 8)
5.0	1.9(-9)	7.2(-10) 1.8(-10)	1.1(-9)	1.3(-8)

B1.3 The Ionization and Dissociation of N_2

The rate coefficient for the ionization is obtained[40] using the measured cross section of Tate and Smith[59] and is given in Table VII.

As for the dissociation of N_2, there exists no direct measurement .

However, a novel method[60] which involves surface adsorption indicates that
the dissociation cross section for 10-300eV electrons is almost as large as
the ionization cross section. The cross sections for dissociation, pre-
dissociation and higher Rydberg states of N_2, whether excited by electron
impact or light absorption, present considerable interest in terms of energy
sink and the product of the dissociation. Some measurements exist[61] for the
products of nitrogen dissociation, mainly in long-lived high Rydberg states
with varying kinetic energy. These measurements are for electron impact
energies of 25eV and higher and would have important implications for
electron excited auroras. It is hoped that more quantitative measurements
for dissociation of N_2 will be available in the near future.

B1.4 <u>Excitations in N_2^+</u>

The nitrogen molecular ion has two low lying electronic states,
$B^2\Sigma$ and $A^2\pi$, which are coupled radiatively to the ground state of the ion.
Two well-known band emissions arise as the result of the excitations of
these states. These are: the Meinel band, $A^2\pi \rightarrow X^2\Sigma$, with emission in
the red and the infrared region of the spectrum, and the first negative
band, $B^2\Sigma \rightarrow X^2\Sigma$, with emission in the blue and the ultraviolet. Because of
the radiative nature and the low threshold energy for their excitations
(see Table II), the B and the A states constitute an important energy sink
for the low energy electrons in the disturbed atmosphere. One of the
strongest bands of the first negative band system is the (0,0) band with its
head at 3914A°. There are several measurements[62-64] for the excitation of
this state. However, there is a large disagreement among the first two
measurements[62,63] and the more recent one[64]. The peak cross sections, as
measured by Lee and Carlton[62] and Dashchenko, et al[63], are 44 and 22 times
as large as that measured by Crandall, et al[64]. A rate coefficient

-22-

measurement by McLean, et al[65], indicated that Lee and Carlton measurement may be large by a factor of 80. It is reasonable, therefore, to assume that the measurement of Crandall, et al[64] provides the best reliable cross section. The rate coefficient for the excitation of the 3914Å band is given in Table VII obtained from Reference 64. Excitation cross section for the A state, from the ground state of the ion has not been measured. However, an estimate for the excitation rate can be obtained using Seaton's cross section for optically allowed transitions and a threshold Gaunt factor of 0.2. The excitation rate coefficient, averaging Seaton's cross section with an electron velocity distribution, is

$$X_{ij} = \frac{1.6 \times 10^{-5} f_{ij} \bar{g}}{\sqrt{T_e}} \, \text{Exp} \, (\Delta E_{ij}/T_e) \qquad (18)$$

Where ΔE_{ij} is the excitation energy that separates states i and j, f_{ij}, the oscillator strength for the transition $(i \rightarrow j)$ and $\bar{g}$ is the average Gaunt factor. In this expression, both ΔE_{ij} and T_e are in units of eV.

B2 Electron Inelastic Collisions in N

Two low lying metastable states, $N(^2D)$, $N(^2P)$, the optically allowed transitions and ionization are the most important energy sinks for the free electrons in nitrogen atom. The metastable $N(^2D)$ holds special significance in the disturbed atmosphere for its rapid reaction with O_2 to form nitric oxide, which in turn emits infrared radiation. The cross sections for the excitation of $N(^2D)$ and $N(^2P)$ from the ground state of nitrogen atom and the excitation of $N(^2P)$ from $N(^2D)$ have been calculated by Seaton[67], Smith, et al[68], Henry, et al[69] and Ormonde, et al[70]. The rate coefficients for the excitations of $N(^2D)$ and $N(^2P)$ reported earlier[40] was obtained using cross sections calculated by Henry, et al[69]. However, a more recent calculation by Berrington, et al[71] includes the polarization of the target

-23-

atom during collision, includes allowance for short range correlation and higher lying configurations. These effects were generally not included in the previous calculations[69]. Therefore, the most recently calculated cross sections[71] are utilized[72] to obtain the excitation rate coefficients of $N(^4S) \rightarrow N(^2D)$, $N(^4S) \rightarrow N(^2p)$ and $N(^2D) \rightarrow N(^2p)$ and are given in Table VIII.

TABLE VIII

Electron Impact Rate Coefficients for the Excitation of Low Lying Metastable, Resonance, ^4p, states and the ionization in N.

T_e(eV)	$^4S - {}^2D$	$^4S - {}^2p$	$^2D - {}^2p$	^4p	Ioniz.
0.1	8.0(-20)	2.6(-25)	2.10(-14)		
0.2	1.54(-14)	2.03(-17)	1.16(-11)		
0.3	1.25(-12)	1.11(-14)	9.78(-11)	1.0(-22)	
0.5	4.2(-11)	1.47(-12)	6.0(-10)	5.0(-17)	7.2(-23)
0.7	1.38(-10)	1.63(-11)	1.16(-9)	1.5(-14)	1.6(-18)
1.0	6.38(-10)	8.91(-11)	2.05(-9)	1.2(-12)	1.6(-15)
1.2	1.08(-9)	1.73(-10)	2.56(-9)	7.0(-12)	2.2(-14)
1.5	1.52(-9)	3.38(-10)	3.24(-9)	4.0(-11)	3.2(-13)
2.0	2.27(-9)	6.54(-10)	4.1(-9)	2.3(-10)	4.9(-12)
3.0	3.31(-9)	1.23(-9)	5.18(-9)	1.5(-9)	7.9(-11)
5.0	4.50(-9)	1.99(-9)	6.2(-9)	7.0(-9)	8.5(-10)

Among the optically allowed transitions, the excitation of the resonance line should constitute an important energy loss for the free electrons. The absolute cross section for the excitation of the upper level of the resonance line, $N(^4p)$ has been measured[73]. Utilizing this cross section, the corresponding excitation rate coefficient as obtained previously[40] is lowered by a factor of three in conformity with the revised cross section for oxygen

resonance line (see Section B4 for detail) is given in Table VIII. As for the ionization rate coefficient given in Table VIII, it was obtained[40] using the measured cross section of Smith, et al[74].

B3 Excitations in N^+ and O^+

The low lying metastable states of N^+ i.e. N^+ (^1D) and N^+ (^1S) and those of O^+ i.e. O^+ (^2D) and O^+ (^2p) are the most important species to consider in the disturbed atmosphere. Their distribution as affected by collisions with electrons, depend on the relevant electron ion collision cross sections. For these species, however, only near threshold collision strengths are calculated. These collision strengths, which are constant over a range of values of interest to the disturbed atmosphere, can be utilized to obtain the relevant deexcitation or excitation rate coeffcients. In Table IX the deexcitation rate coefficients for the low lying metastable states of N^+ and O^+ are presented. The corresponding excitation rate can be obtained using the principle of detailed balance. The collision strengths utilized in Table IX are calculated by Henry, et al[69] for both O^+ and N^+. These calculations[69] agree very well with the calculations for O^+ by Czyzak, et al[75] and the calculations for N^+ by Saraph, et al[76].

-25-

TABLE IX

Deexcitation Rate Coefficients for the Low Lying Metastable States of
O^+ and N^+.

Transition	Deexcitation Rate Coefficient
$^2D - {}^4S$	$\dfrac{1.26 \times 10^{-8}}{\sqrt{T_e}}$
$^2P - {}^4S$	$\dfrac{6.33 \times 10^{-9}}{\sqrt{T_e}}$
$^2P - {}^2D$	$\dfrac{2.36 \times 10^{-8}}{\sqrt{T_e}}$
$^1D - {}^3P$	$\dfrac{4.77 \times 10^{-8}}{\sqrt{T_e}}$
$^1S - {}^3P$	$\dfrac{3.16 \times 10^{-8}}{\sqrt{T_e}}$
$^1S - {}^1D$	$\dfrac{3.28 \times 10^{-8}}{\sqrt{T_e}}$

B4 Electron Inelastic Collisions in O

The excitations of the low lying metastable states, $O(^1D)$, $O(^1S)$, the
optically allowed transitions and the ionization of the atom constitute important
processes that result in the cooling of the free electrons. Measured cross
sections for the low lying metastable states are not available, however,
several calculations exist[68-69,77,78]. The most recent and more accurate
cross sections[77] for $^3p - {}^1D$ and $^1D - {}^1S$ are in good agreement with those of
Henry, et al[69] which were utilized to obtain[40] the relevant excitation cross
sections given in Table X. However, the near threshold behavior for the
excitation of $^3p - {}^1D$ are different between these two calculations[69,77].
The latest cross section calculations[77] were utilized to obtain[72] the

excitation rate coefficient for ^3P - ^1D, given in Table X, which is lower by 20% from the previous rate[40].

The absolute cross section for the excitation of the resonance state ^3S in oxygen was measured along with the resonance state of nitrogen by Stone and Zipf[73]. However, the cross section for the excitation of ^3S state in oxygen was revised as reported in References 79 and 80. This revision, due to some calibration errors, should also be valid for the excitation of the nitrogen resonance state as reported in Section B2. The excitation rate coefficient, given in Table X, reflects this revision from the rate reported previously[40] using the unrevised measured cross section[73]. The ionization rate coefficient for oxygen atom is given in Table X where it was obtained[40] using the measured cross section.

TABLE X

Rate Coefficients for the Excitations of the Low Lying Metastable, Resonance states and the Ionization in 0.

T_e(eV)	^3P - ^1D	^3P - ^1S	^1D - ^1S	^3S	Ioniz.
0.1	1.92 (-18)	1.78 (-28)	2.25 (-19)		
0.2	5.28 (-14)	1.96 (-19)	1.76 (-14)		
0.3	1.76 (-12)	2.10 (-16)	8.07 (-13)	1.5 (-22)	
0.5	3.28 (-11)	6.04 (-14)	1.52 (-11)	4.2 (-17)	1.55 (-20)
0.7	1.21 (-10)	7.25 (-13)	5.4 (-11)	1.0 (-14)	3.8 (-17)
1.0	3.43 (-10)	4.93 (-12)	1.38 (-10)	6.5 (-13)	1.4 (-14)
1.2	5.20 (-10)	1.06 (-11)	1.97 (-10)	3.3 (-12)	1.4 (-13)
1.5	7.94 (-10)	2.32 (-11)	2.76 (-10)	1.7 (-11)	1.5 (-12)
2.0	1.21 (- 9)	5.15 (-11)	3.98 (-10)	9.0 (-11)	1.62 (-11)
3.0	1.84 (- 9)	1.16 (-10)	5.30 (-10)	5.0 (-10)	1.9 (-10)
5.0	2.52 (- 9)	2.21 (-10)	7.16 (-10)	1.6 (- 9)	1.6 (- 9)

B5 Electron Inelastic Collisions in 0_2

In contrast with N_2 where a large number of measurements and calculations exist for several of its electronic states, the oxygen molecule fairs poorly in this aspect. The cross sections for the excitations of $a^1\Delta$ and $b^1\Sigma$ have been measured[83] and a calculation[84] exists for the excitation of $a^1\Delta$. The agreement between the measured and calculated cross sections is very poor near threshold: This should be expected since the calculation is a Born-type approximation where it is valid for high incident electron energy. Indeed the agreement between experimental[83] and the calculated[84] cross section for $a^1\Delta$ is very good at higher energies. Using the measured cross sections[83], the respective excitation rate coefficients are given in Table XI. Two important electronic states, one forbidden $A^3\Sigma$ and the other allowed $B^3\Sigma$,

-28-

whose excitations lead to the dissociation of the molecule, have no measured or calculated values. However, using the generalized oscillator strengths obtained from electron energy loss spectrums in 0_2, analytic expressions[84,85] for $A^3\Sigma$, $B^3\Sigma$ states exist along with other electronic states[84,85]. Using the parameters given in Reference 85, we have obtained the cross sections for $A^3\Sigma$ and $B^3\Sigma$ states in 0_2. Using the threshold values of these cross sections, we have obtained the electron impact excitation rate coefficients of the states $A^3\Sigma$ and $B^3\Sigma$. These rates are given in Table XI for low energy incident electrons.

In addition to the rates discussed above, we give in Table XI the electron impact ionization rate coefficient for 0_2. This rate is obtained[40] using the measured cross section[59].

TABLE XI

Electronic Excitation and Ionization Rate Coefficients in 0_2

T_e	$a(^1\Delta)$	$b^1\Sigma$	$A^3\Sigma$	$B^3\Sigma$	Ioniz.
0.1	1.7 (-15)	3.1 (-18)			
0.2	5.1 (-13)	1.6 (-14)			
0.3	3.7 (-12)	3.2 (-13)	2.3 (-15)	2.9 (-22)	1.7 (-28)
0.5	2.3 (-11)	4.1 (-12)	1.3 (-12)	3.3 (-17)	1.2 (-20)
0.7	3.2 (-11)	1.4 (-11)	2.1 (-11)	5.3 (-15)	3.0 (-17)
1.0	1.3 (-10)	3.2 (-11)	1.9 (-10)	2.6 (-13)	1.1 (-14)
1.2	1.9 (-10)	4.6 (-11)	4.7 (-10)	1.2 (-12)	1.2 (-13)
1.5	3.0 (-10)	6.7 (-11)	1.2 (-9)	5.8 (-12)	1.25 (-12)
2.0	4.4 (-10)	1.1 (-10)	3.4 (-9)	3.0 (-11)	1.3 (-11)
3.0	6.5 (-10)	1.5 (-10)	1.0 (-8)	1.8 (-10)	1.6 (-10)
5.0	8.5 (-10)	2.0 (-10)	3.5 (-8)	9.0 (-10)	1.13 (-9)

C Charge Exchange, Ion-Molecule Rearrangement, Neutral Particle Reactions
and Quenching Reactions

The deionization processes in the disturbed atmosphere are controlled by
a large number of reactions that include charge exchange, ion-molecule
rearrangement, neutral particle reactions and neutral quenching reactions.
These reactions in general, play an important but indirect role in the
deionization. They affect the vibrational temperature of molecules and their
ions, the translational temperatures of the heavy particles and emission from
molecules and their ions.

C1 Charge Exchange Reactions

The charge exchange between an atomic ion and a molecule, for example,
converts the atomic ion into a molecular ion which has a much faster rate in
recombining dissociatively with the free electrons. Some of these charge
exchange processes are near resonance and thus proceed at a much faster rate
in comparison with the nonresonant process. In addition to the conversion of
the atomic ion into a molecular ion, occasionally the near resonance charge
exchange[86] process results in emission from the excited states of the
molecular ions. Two examples of such reactions are

$$O^+(^2D) + N_2 \rightarrow N_2^+(A^2\pi) + O \qquad (19)$$

$$O^+(^2D) + O_2 \rightarrow O_2^+(A^2\pi) + O \qquad (20)$$
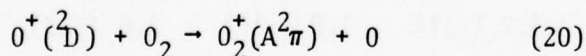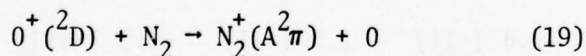
where emission may result in the infrared and the visible. A host of charge
exchange reactions that occur in the disturbed E and F regions with their
rate coefficients are given in Table XII along with the reference to the source
of the rate coefficient.

TABLE XII

Charge Exchange Reactions

Symbol	Reaction	Rate Coefficient	Ref.
C_1	$N_2^+ + O \rightarrow N_2 + O^+$	(a) $4.22 \times 10^{-12} \, (T_a)^{-0.23}, T_a \leq 0.13$ eV	87
		(b) $1.62 \times 10^{-11} \, (T_a)^{0.41}, T_a > 0.13$ eV	
C_2	$N_2^+ + O_2 \rightarrow N_2 + O_2^+$	(a) $2.7 \times 10^{-12} \, (T_a)^{-0.8}, T_a \leq 0.3$	88
		(b) $4.2 \times 10^{-11} \, (T_a)^{1.4}, T_a > 0.3$	
C_3	$N_2^+ + N \rightarrow N_2 + N^+$	$<10^{-11}$	89
C_4	$N_2^+ + NO \rightarrow N_2(A) + NO^+$	3.3×10^{-10}	89,90
C_5	$O^+(^2D) + N_2 \rightarrow N_2^+(A) + O$	$(3-9) \times 10^{-10}$	91
C_7	$N^+ + O \rightarrow O^+ + N$	$\leq 10^{-12}$	89
C_8	$N^+ + O_2 \rightarrow O_2^+ + N$	(a) $2.8 \times 10^{-10} \, T_a \leq 0.39$	88,89
		(b) $4.8 \times 10^{-10} \, (T_a)^{0.57}, T_a > 0.39$	
C_9	$N^+ + NO \rightarrow N + NO^+$	8×10^{-10}	89
C_{13}	$O^+ + O_2 \rightarrow O_2^+ + O$	(a) $4.6 \times 10^{-12} \, (T_a)^{-0.4}, T_a \leq 0.155$	18,88
		(b) $1.0 \times 10^{-10} \, (T_a)^{1.2}, T_a > 0.155$	
C_{13a}	$O^+(^2D) + O_2 \rightarrow O_2^+ + O$	3×10^{-10}	92
C_{19}	$O_2^+ + NO \rightarrow O_2 + NO^+$	4.4×10^{-10} at $300k°$	93
C_{19a}	$O_2^+(a^4\pi) + NO \rightarrow O_2 + NO^+$	1.1×10^{-9}	93
CE_1	$O^+ + NO \rightarrow NO^+ + O$	(a) $7.5 \times 10^{-13}, .025 \leq T_a \leq 0.1$	94,95
		(b) $3.2 \times 10^{-11} \, (T_a)^{1.38}, T_a > 0.1$	
	$O^+(^2D) + NO \rightarrow NO^+ + O$	40 times larger then CE_1	96
CE_3	$O_2^+(a^4\pi) + N_2 \rightarrow N_2^+ + O_2$	4.1×10^{-10} at $300k°$	93
	$O_2^+(a^4\pi) + O_2 \rightarrow O_2^+(x) + O_2$	3.1×10^{-10} constant up to 1.4 ev	

C2 Ion-Molecule Rearrangement Reactions

The ion-atom interchange in the ion-molecule rearrangement reactions results in the conversion of an atomic ion into a new molecular ion, or an atomic ion and a new molecule. Reactions that result in a new molecular ion generally enhances the deionization process. In many of these reactions, the vibrational state of the resulting molecular ion is not known. However, the reactions are exothermic with sufficient energy to excite a large number of vibrational states and thus contribute to infrared emission. In Table XIII are given relevant ion-atom interchange reactions with their rate coefficients and the source of the rate coefficient.

TABLE XIII

Ion-Atom Interchange Reactions

| Symbol	Reaction	Rate Coefficient	Ref.
C_6	$N_2^+ + 0 \rightarrow N0^+ + N$	(a) $2.8 \times 10^{11}(T_a)^{-0.44} - 4.22 \times 10^{12}(T_a)^{-0.23}, T_a \leq 0.13$	87
		(b) $1.1 \times 10^{10}(T_a)^{0.2} - 1.62 \times 10^{11}(T_a),^{0.41} T_a > 0.13$	
C_{10}	$0_2^+ + N \rightarrow N0^+ + 0$	1.2×10^{-10}	97
C_{11}	$N^+ + 0_2 \rightarrow N0^+ + 0$	(a) $2.8 \times 10^{10}, T_a \leq 0.39$	88
	$\rightarrow 0_2^+ + N$	(b) $4.8 \times 10^{10}(T_a)^{0.57} T_a > 0.39$	
K_{Tv}	$0^+ + N_2 \rightarrow N0^+ + N$	(a) $3.1 \times 10^{14}(T_a)^{-1.0}, T_a \leq 0.065$	
		(b) $1.2 \times 10^{10}(T_a)^{2.0}, 0.67 \geq T_e \geq 0.065$	18,88
		(c) $8.5 \times 10^{11}(T_a)^{1.2}, T_a > 0.67, T_a = T_v$	

C3 Neutral Particle Reactions and Neutral Quenching

When energy is deposited in the atmosphere, several metastable neutral species are formed. Some of these species emit radiation in the visible or the infrared whose magnitude and duration are of special significance for

systems, as well as the relaxation of the disturbed atmosphere. The time histories of these species are controlled by charge particle reactions (electrons and ions) and collisions with neutral particles. Among the neutral particle reactions of significance are the quenching reactions which affect the metastable species, and the atom-atom interchange that affects the formation and destruction of N0. In Table XIV are given some relevant neutral particle collisions with their respective rate coefficients and the source of these coefficients.

D Associative Ionization

In air at temperatures of 0.1 eV and higher, ionization proceeds through associative ionization. One of the associative ionizations of interest to the E and F regions is

$$N + 0 \rightarrow N0^+ + e \qquad (21)$$
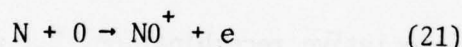
This reaction has been observed in shock heated plasmas[27]. Associative ionizations leading to N_2^+ and 0_2^+ through the reactions of two nitrogen and two oxygen atoms, respectively, also proceed in shock heated plasmas, however, they require higher particle energies or higher temperatures. Reaction (21) on the other hand, requires an activation energy of 2.8 eV. For applications to the disturbed E and F regions, however, the following reaction

$$N(^2D) + 0 \rightarrow N0^+ + e \qquad (22)$$
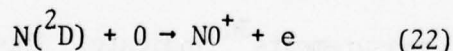
is of more interest, especially since its activation energy is ~ 0.43 eV. Lin and Teare[27] have obtained the equilibrium constant for reaction (23) and give the following expression

$$K_e = (1.62\ T_a + 1.61\ T_a^2 + 2.2\ T_a^3) \times 10^{-4} \cdot \exp(-\frac{2.8}{T_a}) \qquad (23)$$

with an accuracy of + 20% in the temperature range of 0.025 - 2.6 eV. One can obtain the equilibrium constant for reaction (22), K_{34}^e, using the expression given in Equation (23); that is

$$K_{34}^e = K_e \cdot \frac{N}{N(^2D)} \qquad (24)$$

where

$$N(^2D) = \frac{g(^2D)}{P(T_a)} N \, Exp(-2.37/T_a) \qquad (25)$$

Here, $g(^2D)$ and $P(T_a)$ are the statistical weight of ^2D state and the partition function of the nitrogen atom. Using relations (24) and (25), one obtains

$$K_{34}^e = K_e \cdot \frac{P(T_a)}{g(^2D)} \, Exp(2.37/T_a) \qquad (26)$$

Thus, an approximate expression for the equilibrium constant for reaction (22), K_{34}^e, is

$$K_{34}^e = K_e \cdot [0.4 \, Exp(\frac{2.37}{T_a}) + 1] \qquad (27)$$

where only the first two terms of the partition function, $P(T_a)$, are utilized: Thus, the rate coefficient for the forward reaction (22) can be obtained using relation (27) and the rate coefficient for the reverse reaction i.e., the dissociative recombination, D_2, as given in Table III. We select the following expression for D_2

$$D_2 = 9.8 \times 10^{-8} \, (T_e)^{-0.37} \qquad (28)$$

as obtained from measurements of Huang, et al[23], which differs from the measurements of Walls and Dunn[22]. The discrepancy between these two measurements may be due to the presence of resonances[104] in the dissociative recombination cross section. We assume that reaction (28) leads into $N(^2D)$ and 0 as calculations[29] and measurements[30] indicate. Thus,

$$K_{34} = 9.8 \times 10^{-12}(T_e)^{-0.37}[0.4 \, Exp(-0.43/T_a) + Exp(-2.8/T_a)] \times$$
$$[1.62 \, T_a + 1.61 \, T_a^2 + 2.2 \, T_a^3] \qquad (29)$$

This should be compared with the following expressions obtained by Baurer[105] for the forward reaction in (22):

$$K_{34} = 7.6 \times 10^{-13}(\frac{T}{0.025})^{0.6} \, Exp(-0.43/T_a) \ ; \ T_a \leq 0.172 \, eV$$

and $\qquad (30)$

$$K_{34} = 3.1 \times 10^{-13}(\frac{T_a}{0.025})^{1.1} Exp(-0.43/T_a) \ , \ 0.172 \leq T_a \leq 0.51 \, eV$$

Baurer[105] has obtained these expressions using D_2 as given by Equation
(28) [with T_e to the power of (-0.4)] and a calculated equilibrium constant.
A comparison of the two expressions (29) and (30) show that the agreement
between them is good where they differ from each other by only 20%.

TABLE XIV

Neutral Particle and Quenching Reactions

Symbol	Reaction	Rate Coefficient	Ref.
C_{14}	$N(^2D)+O_2 \to NO+N$	$4.7 \times 10^{-11} \sqrt{T_a}$	98, 100
C_{15}	$O+N_2 \to NO+N$	$1.3 \times 10^{-10} \text{Exp}(\frac{-3.27}{T_a})$	89
C_{16}	$N+NO \to N_2+O$	$8.2 \times 10^{-11} \text{Exp}(\frac{-0.035}{T_a})$	89
C_{17}	$N+O_2 \to NO+O$	$1.3 \times 10^{-10} T_a \text{ Exp}(\frac{-0.27}{T_a})$	89
C_{18}	$O+NO \to O_2+N$	$2.9 \times 10^{-11} T_a \text{ Exp}(\frac{-1.68}{T_a})$	89
C_{20}	$N_2(A)+O \to O(^1S)+N_2$	3.0×10^{-12}	99
C_{21}	$N(^2D)+N_2 \to N+N_2$	1.6×10^{-14}	100
C_{22}	$N(^2D)+NO \to N+NO$	7×10^{-11}	100
C_{22a}	$N(^2D)+O \to N+O$	1.8×10^{-12}	101
C_{23}	$O+O+O \to O(^1S)+O_2$	1.5×10^{-34}	102
C_{24}	$O(^1D)+N_2 \to O+N_2$	5.5×10^{-11}	103
C_{25}	$O(^1D)+O_2 \to O+O_2(^1\Sigma)$	7.5×10^{-11}	103
C_{26}	$O(^1S)+O_2 \to O+O_2$	$4.3 \times 10^{-12} \text{Exp}(\frac{-0.07}{T_a})$	103
C_{27}	$O(^1S)+O \to O+O$	7.5×10^{-12}	103
C_{28}	$O(^1S)+NO \to O+NO$	5.5×10^{-10}	103
C_{29}	$O(^1D)+NO \to NO+O$	2.1×10^{-10}	103
C_{30}	$N_2(A)+N \to N_2+N$	5×10^{-11}	89
C_{31}	$N_2(A)+O_2 \to N_2+O_2$	3.8×10^{-11}	89

E Additional Reactions in the Disturbed E and F Regions

In the disturbed E and F regions of the ionosphere, a large number of excited states are formed. These states are neutral or ionic in nature (see Table I). They clearly play an important role in the emission and the deionization of the disturbed region. However, there are a number of reactions that may occur between the excited species, and between them and the neutral species whose reaction rates are not known but could be large in comparison with similar reactions with reactants being in the ground state. In this section, we present a list of such reactions which fall in the category of the charge exchange and ion-molecule rearrangements. These reactions are energetically possible with the total spin being conserved, and are a partial list of a larger set discussed elsewhere[106]. This list is chosen here because of the near resonance nature of the reactions where the energy defect is small. Furthermore, a careful examination of these reactions will reveal their obvious impact on the emission and the deionization where emission is alternated from one frequency to another and an atomic ion is replaced by a molecular one. The reactions of interest are:

Reaction	Excess Energy
$N_2^+(^2\Sigma) + O(^1D) \rightarrow N_2(^1\Sigma) + O^+(^2D)$	0.60
$N_2^+(^2\Sigma) + O_2(^1\Sigma) \rightarrow N_2(^1\Sigma) + O_2^+(A^2\pi)$	0.32
$N_2^+(^2\Sigma) + N(^2D) \rightarrow N_2(^1\Sigma) + N^+(^1D)$	0.53
$N_2^+(^2\Sigma) + N(^2P) \rightarrow N_2(^1\Sigma) + N^+(^1S)$	0.57
$N_2^+(^2\Sigma) + O(^3P) \rightarrow NO^+(^1\Sigma) + N(^2D)$	0.69
$N^+(^3P) + O(^1D) \rightarrow N(^2D) + O^+(^4S)$	0.5
$N^+(^1D) + O(^3P) \rightarrow N(^2D) + O^+(^4S)$	0.43
$N^+(^3P) + O_2(^3\Sigma) \rightarrow O_2^+(^2\pi) + N(^2D)$	0.10

Reaction	Excess Energy
$N^+(^3P) + O_2(^1\Sigma) \rightarrow O_2^+(^4\pi) + N(^4S)$	0.03
$N^+(^1D) + O_2(^3\Sigma) \rightarrow O_2^+(^2\pi) + N(^2P)$	0.79
$N^+(^1D) + O_2(^3\Sigma) \rightarrow O_2^+(^4\pi) + N(^4S)$	0.36
$N^+(^1S) + O_2(^3\Sigma) \rightarrow O_2^+(^4\Sigma) + N(^4S)$	0.38
$N^+(^1S) + O_2(^1\Sigma) \rightarrow O_2^+(A^2\pi) + N(^2D)$	0.95
$N^+(^3P) + NO(^2\pi) \rightarrow NO^+(^3\Sigma) + N(^4S)$	0.13
$N^+(^1S) + NO(^2\pi) \rightarrow NO^+(^3\Sigma) + N(^2P)$	0.81
$N^+(^3P) + O_2(^1\Delta) \rightarrow NO^+(^3\Sigma) + O(^1D)$	0.69
$N^+(^1S) + O_2(^1\Delta) \rightarrow NO^+(^1\pi) + O(^1D)$	0.71
$N^+(^1D) + O_2(^3\Sigma) \rightarrow NO(^2\pi) + O^+(^2D)$	0.89
$N^+(^3P) + O_2(^1\Delta) \rightarrow NO(^2\pi) + O^+(^2D)$	0.0
$N^+(^3P) + O_2(^1\Sigma) \rightarrow NO(^2\pi) + O^+(^2D)$	0.6
$N^+(^1D) + O_2(^1\Sigma) \rightarrow NO(^2\pi) + O^+(^2P)$	0.8
$O^+(^2D) + O_2(^3\Sigma) \rightarrow O(^3P) + O_2^+(A^2\pi)$	0.08
$O^+(^2D) + O_2(^3\Sigma) \rightarrow O(^3P) + O_2^+(^4\pi)$	0.88
$O^+(^2D) + O_2(^3\Sigma) \rightarrow O(^1S) + O_2^+(^2\pi)$	0.70
$O^+(^2P) + O_2(^3\Sigma) \rightarrow O(^1D) + O_2^+(^4\pi)$	0.61
$O^+(^2P) + O_2(^1\Delta) \rightarrow O(^1D) + O_2^+(A^2\pi)$	0.81
$O^+(^2D) + O_2(^1\Sigma) \rightarrow O(^3P) + O_2^+(^4\Sigma)$	0.34
$O_2^+(^4\pi) + NO(^2\pi) \rightarrow O_2(B^3\Sigma) + NO^+(^1\Sigma)$	0.0
$O^+(^2D) + N_2(^1\Sigma) \rightarrow NO^+(^1\Sigma) + N(^2P)$	0.85

Reaction	Excess Energy
$O^+(^2D) + NO(^2\pi) \rightarrow NO^+(^3\Sigma) + O(^1D)$	0.49
$O^+(^2P) + NO(^2\pi) \rightarrow NO^+(^3\Delta) + O(^1D)$	0.11
$O^+(^2P) + NO(^2\pi) \rightarrow NO^+(^1\pi) + O(^3P)$	0.3
$O^+(^4S) + NO(^2\pi) \rightarrow O_2^+(^2\pi) + N(^4S)$	0.15

It should be remarked that the excess energy (the energy defect) in most of these reactions may end up in the vibrational excitations of the end products of the reactions whenever there are molecules or molecular ions, thus making the reaction a resonance reaction which generally has a large rate coefficient.

V The electron, N_2 Vibrational and Heavy Particle Temperatures

From the preceeding sections, the dependence of the reaction rates on several temperatures is obvious. Therefore, the description of the time histories of the species and their emission requires the calculation of the relevant temperature that enters in each reaction.

A The Electron Temperature

The electron gains energy primarily during the energy deposition phase and loses its energy continuously through elastic and inelastic collisions with the species of the disturbed region. The inelastic collisions include the ionization and the excitations of the internal degrees of motion of the individual species. Among these are the excitations of the electronic states of the atoms, molecules and their ions, and the vibrational excitations of the molecular species. However, part of the excitation energies expended in the excitations of the metastable electronic states and the vibrational levels, is returned to the electron gas through the superelastic collisions. Most of these processes and their respective rate coefficients were presented in Section IV.

The electrons share their energies with ions with an equipartition time[107]

-39-

of

$$T_{eq} = 5.87 \frac{A_e A_i}{N_i \log \Lambda} \left(\frac{T_e}{A_e} + \frac{T_i}{A_i} \right)^{3/2} \qquad (31)$$

where N_i is the ion density and $\log \Lambda$ for E and F regions is of the order of (20-30), A_e and A_i are the atomic weights of the electron ($\frac{1}{1843}$) and of the ion, respectively. Thus a term in the electron temperature equation using (21) would be

$$\frac{dT_e}{dt} = -2.3 \times 10^{-8} \frac{N_i}{A_i} \frac{T_e - T_a}{T_e^{3/2}} \qquad (32)$$

to describe the loss to ions.

B N_2 Vibrational Temperature

One of the important processes that affects the removal of the electrons in late times, when the disturbed region is not completely ionized, is

$$O^+ + N_2^+ \rightarrow NO^+ + N \qquad (33)$$

In this reaction NO^+ is formed which in turn dissociatively recombines with the free electrons at a rapid rate. The formation of NO^+ depends on the kinetic temperature of O^+ as well as the vibrational temperature. Therefore, the calculation of the N_2 vibrational temperature is required to provide the appropriate rate coefficient for reaction (33). The vibrational of the nitrogen molecule arises from several mechanisms. These are: the electron impact excitation[34,35]

$$e + N_2 \rightarrow N_2^{\mp} + e, \qquad (34)$$

the electronic energy transfer[108,109]

$$O(^1D) + N_2 \rightarrow N_2^{\mp} + O(^3P), \qquad (35)$$
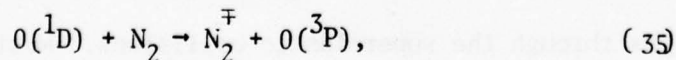
the atom-atom interchange[110,111]

$$N + NO \rightarrow N_2^{\mp} + O \qquad (36)$$

and charge exchange

$$N_2^+ + O \rightarrow N_2^{\mp} + O^+ \qquad (37)$$

$$N_2^+ + O_2 \rightarrow N_2^{\mp} + O_2^+ \qquad (38)$$

$$N_2^+ + N \rightarrow N_2^{\mp} + N^+ \qquad (39)$$

$$N_2^+ + NO \rightarrow N_2(A) + NO^+ \qquad (40)$$

These last reactions (37-40) are all exothermic and the excess energy may end up either kinetic or vibrational energy or both. Reaction (40) contributes to the vibrational energy of the nitrogen ground state via cascade from A to X state as would other electronic excitations of N_2. However, no m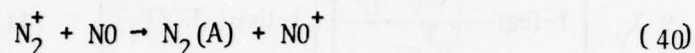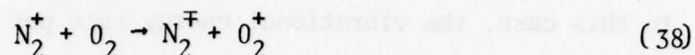easurement or calculations are avilable for these reactions. Finally, in reaction (36) if the atomic nitrogen was in ^2D state, higher vibrational levels of N_2 may be excited.

Among the preceeding reactions leading to the vibrational excitation of N_2, the electron impact excitation is well understood and has reliably measured cross sections[34].The electronic energy transfer from $O(^1D)$ which is in resonance with the seventh vibrational level, has been calculated[106,107] with different results. Fisher and Bauer[108] indicated that only 5% of the electronic energy is transferred into vibrational energy. However, calculations by Black[109] indicates that 30% of the electronic energy is converted into vibrational energy. As for reaction (36), it has been found[110] that approximately a quarter of its excess energy ends up in the vibrational energy of N_2, thus exciting up to v=3.

The reduction of the vibrational energy proceeds via the deexcitation of the vibrational levels by electron collisions and the deactivation of the molecule by oxygen atom which apparently depends on the kinetic temperature[112,114].

When the dominant mechanism of the vibrational excitation is electron

impacts, the vibrational temperature can be calculated[3] assuming that the molecule is a harmonic oscillator and that the vibrational levels have a Boltzman distribution. In this case, the vibrational energy rate per molecule due to an electron density of N_e, is

$$\frac{dEv}{dt} = N_e E_1 \sum_{v=1}^{8} v X_v \left[1 - Exp \frac{vE_1(T_v - T_e)}{T_v T_e} \right] \left[1 - Exp(-E_1/T_v) \right] \quad (41)$$

with

$$E_v = \frac{E_1}{Exp(E_1/T_v) - 1} \quad (42)$$

where, as usual, T_e and T_v stand for KT_e and KT_v, respectively, X_v is the excitation rate coefficient for the vth vibrational level and are given in Table IV. And E_1 is the vibrational energy spacing which is ~ 0.3 eV for N_2 molecule. The above relation (Eq. 41) is obtained using a rate equation approach where one could incorporate other vibrational excitation and deexcitation processes discussed in this section.

C Heavy Particle Temperature

The heavy particles include charged and neutrals. Their kinetic energy arises from the dissociation of the molecules, the dissociative recombination of the molecular ions, the charge exchange and the rearrangement collisions, quenching of internal energies of the species and by the electron ion collisions (See Eq. 32).

The amount of energy released to the heavy particle through the dissociative recombinations is well understood, especially since the products of the recombinations are reasonably well established. However, the amount of energy released as kinetic in charge exchange and rearrangement collisions remains unresolved, since the exothermic energy may be partitioned among other degrees

-42-

of freedom. It could be assumed, however, that all excess energies of these reactions end up as kinetic. In Table XV, a list of the exothermicity of the reactions involved in the disturbed region is identified. However, if one assumes[104] that a much larger set of reactions in the arena of charge exchange and rearrangement collisions is possible, then a different set of exothermic energies will arise[106].

TABLE XV

Exothermic Energies of Reactions Heating the Heavy Particles

Reaction Identified by Their Coefficient	Exothermic Energy (eV)
D_1	3.45
D_2	0.39
D_3	4.78
C_1	1.96
C_2	3.52
C_3	1.04
C_4	0.0
C_5	0.0
C_6	3.06
C_7	0.92
C_8	2.48
C_9	5.27
C_{10}	4.20
C_{11}	6.67
C_{12}	2.32
C_{13}	1.56
C_{13a}	0.0
C_{14}	2.77

Reaction Identified by Their Coefficient	Exothermic Energy (eV)
C_{15}	-3.25
C_{16}	3.25
C_{17}	1.4
C_{18}	-1.4
C_{19}	2.79
C_{19a}	6.79
K_{IV}	1.10
C_{21}	2.37
C_{22}	2.37
C_{22a}	2.37
C_{24}	1.96
C_{26}	4.16
C_{27}	4.16
C_{28}	4.16
C_{29}	1.96
C_{30}	6.0
C_{31}	6.0
CE_1	4.3

REFERENCES

1. A. W. Ali, "Electron Pressure Profile in the F-Layer UV-Fireball", Plasma Dynamics Tech. Note 20, Plasma Physics Division, NRL (1969)

2. A. W. Ali, "The Chemistry and the Rate Coefficients of the F-Layer UV-Fireball, Plasma Dynamics Tech. Note 24, Plasma Physics Division, NRL (1970)

3. A. W. Ali, "The Physics and Chemistry of Two NRL Codes for the Disturbed E and F Regions", NRL Report 7578 (1973)

4. A. W. Ali, A. D. Anderson and E. Hyman, "Two Late-Time Deionization Codes", Proceedings of High Altitude Nuclear Effects Symposium, Vol. 2 DASIAC SR-130, Dec. 1971

5. F. R. Gilmore, J. Quant. Spectrosc. Radiat. Transfer 5, 369 (1965)

6. D. E. Shemansky and N. P. Carleton, J. Chem. Phys. 51, 682 (1969)

7. R. W. B. Pearse and A. G. Gaydon, "The Identification of Molecular Spectra", 3rd Ed. Chapman and Hall   London (1965)

8. R. M. Badger, A. C. Wright and R. F. Whitlock, J. Chem. Phys. 43, 4345 (1965)

9. J. H. Miller, R. W. Boese and L. P. Giver, J. Quant. Spectrosc. Radiat. Transfer 9, 1507 (1969)

10. J. William McGowan, R. H. Kummler and F. R. Gilmore, Defense Nuclear Agency Reaction Rate Handbook 2nd Ed. M. Bortner and T. Baurer Eds. Chap. 20, GE TEMPO (1972)

11. W. L. Wiese, M. W. Smith and B. M. Glennon, "Atomic Transition Probabilities", Vol. 1 NBS (1966)

12. J. R. Peterson and J. T. Moseley, J. Chem. Phys. 58, 172 (1973)

13. C. E. Head, Phys. Lett. 34A, 92 (1971)

14. W. F. Sheridan, O. Oldenberg and N. P. Carleton, in Atomic Collision

Processes, M. R. C. McDowell, Ed. (North-Holland-Amsterdam 1964) p. 440

15. M. A. Biondi, Can. J. Chem. $\underline{47}$, 1711 (1969)

16. D. R. Bates and A. Dalgarno, Chapter 7 in "Atomic and Molecular Processes"
    Bates Ed. Academic Press, New York (1962)

17. A. L. Schmeltekopf, F. C. Fehsenfeld, G. I. Gilman and E. E. Ferguson,
    Planet Spac. Sci. $\underline{15}$, 401 (1967), A. L. Schmeltekopf, E. E. Ferguson and
    F. C. Fehsenfeld, J. Chem. Phys. $\underline{48}$, 2966 (1968)

18. R. Johnsen and M. A. Biondi, J. Chem. Phys. $\underline{59}$, 3504 (1973)

19. T. F. O'Malley, Phys. Rev. $\underline{185}$, 101 (1969)

20. T. F. O'Malley, A. J. Cunningham and R. M. Hobson, J. Phys. B - Atomic and
    Molecular Phys. $\underline{5}$, 2126 (1972)

21. F. J. Mehr and M. A. Biondi, Phys. Rev. $\underline{181}$, 264 (1969) and references
    therein

22. F. L. Walls and G. H. Dunn, J. Geophys. Res. $\underline{79}$, 1911 (1974)

23. C. M. Huang, M. A. Biondi and R. Johnsen, Phys. Rev. A$\underline{11}$, 901 (1975)

24. M. A. Biondi, Chapter 11 DASA Reaction Rate Handbook 1948, (1967)

25. R. C. Gunton and T. M. Shaw, Phys. Rev. $\underline{140}$, A748 (1965)

26. C. S. Weller and M. A. Biondi, Bull. Am. Phys. Soc. $\underline{11}$, 495 (1966)

27. S. C. Lin and J. D. Teare, Phys. Fluids $\underline{6}$,   355 (1963)

28. A. W. Ali, "The Influence of the Dissociative Recominations Products on
    the Disturbed F-Layer Electron Density", Plasma Dynamics Technical
    Note 32, (1970)

29. H. H. Michels, "Theoretical Study of Dissociative Recombination Kinetics"
    AFWL-TR-73-288 (1974)

30. D. Kley, G. M. Lawrence and E. J. Stone, J. Chem. Phys. $\underline{66}$, 4157 (1977)

31. H. H. Michels, H. J. Kolker and G. Peterson, "Theoretical Analysis of
    Dissociative Recombination in N_2^+", Proceedings of High Altitude Nuclear

Effects Symposium SRI, August (1971)

32. E. C. Zipf, (Abstract) Bull. Am. Phys. Soc. 15, 418 (1970)

33. A. W. Ali, Appl. Optics 8, 993 (1969)

34. G. J. Schulz, Phys. Rev. 116, 1141(1959) Ibid 125, 229 (1962), 135, A988 (1964)

35. H. Ehrhardt and K. Willmann, Z. Physik 204, 462 (1967)

36. A. Herzenberg and F. Mandl, Proc. Roy. Soc. A270, 48 (1962)

37. J. C. Y.Chen, J. Chem. Phys. 40, 3507 (1964)

38. D. T. Britwistle and A. Herzenberg, J. Phys. B4, 153 (1971)

39. G. J. Schulz, Rev. Mod. Phys. 45, 378 (1973)

40. A. W. Ali and A. D. Anderson, "Low Energy Electron Impact Rate Coefficients for Some Atmospheric Species", NRL Report 7432 (1972)

41. D. E. Shemansky, J. Chem. Phys. 51, 689 (1969)

42. J. A. Meyer, D. W. Setser and D. H. Stedman, Astrophys. J. 157, 1023 (1969)

43. J. William McGowan, R. H. Kummler and F. R. Gilmore, Chapt. 20, "DNA Reaction Rate Handbook", DNA 1948H, Bortner and Baurer Eds. Published by DASIAC DoD Nuclear Information and Analysis Center 1972

44. D. C. Cartwright, Aerospace Report No. TR-0059 (9260-01)-6 The Aerospace Corporation, El Segundo, CA, August (1970) and Phys. Rev. A2, 1331 (1970)

45. S. Chung and C. C. Lin, Phys. Rev. A6, 988 (1972)

46. R. T. Brinkmann and S. Trajmar, Ann. Geophys. 26, 201 (1970)

47. W. L. Borst, Phys. Rev. A5, 648 (1972)

48. P. N. Stanton and R. M. St. John, J. Opt. Soc. Am. 59, 252 (1969)

49. D. E. Shemansky and A. L. Broadfoot, J. Quant. Spect. Rad. Transfer 11, 1401 (1971)

50. J. D. Jobe and F. A. Sharpton and R. M. St. John, J. Opt. Soc. Am. 57, 106 (1967)

51. D. J. Burns, F. R. Simpson and J. W. McConkey, J. Phys. $\underline{B2}$, 52 (1969)

52. V. V. Skubenich and I. P. Zapesochny, Fifth Int. Conf. on Physics and Atomic Collisions, Leningrad, U.S.S.R. (1967) (Nauka Publishing House, Leningrad 1967), p. 570

53. R. S. Freund, J. Chem. Phys. $\underline{54}$, 1407 (1971)

54. A. W. Ali, "Auroral Emission and Inelastic Electron Collision Processes in Air", NRL Memo Report 2742 (1973)

55. J. Ajello, J. Chem. Phys. $\underline{53}$, 1156 (1970)

56. J. F. M. Aarts and F. J. DeHeer, Physica $\underline{52}$, 45 (1971)

57. R. F. Holland, J. Chem. Phys. $\underline{51}$, 3940 (1969)

58. T. G. Finn and J. P. Doering, J. Chem. Phys. $\underline{64}$, 4490 (1976)

59. J. T. Tate and P. T. Smith, Phys. Rev. $\underline{39}$, 270 (1932)

60. H. F. Winters, J. Chem. Phys. $\underline{44}$, 1472 (1966)

61. W. C. Wells, W. L. Borst and E. C. Zipf, Phys. Rev. A $\underline{14}$, 695 (1976)

62. A. R. Lee and N. P. Carleton, Phys. Lett. A $\underline{27}$, 195 (1968)

63. A. I. Dashchenko, I. P. Zapesochny, and A. I. Imre, Opt. Spectrosk. $\underline{35}$, 970 (1973)

64. D. H. Crandall, W. E. Kauppila, R. A. Phaneuf, P. O. Taylor and G. H. Dunn, Phys. Rev. A $\underline{9}$, 2545 (1974)

65. E. A. McLean, A. W. Ali, J. A. Stamper, S. O. Dean, Phys. Lett. A $\underline{38}$, 209 (1972)

66. M. J. Seaton, in "Atomic and Molecular Processes", Bates Ed. (Academic Press, Inc., New York 1962)

67. M. J. Seaton, in "The Airglow and the Aurorae", Armstrong and Dalgarno, Eds., London (1956)

68. K. Smith, R. J. W. Henry and P. G. Burke, Phys. Rev. $\underline{157}$, 51 (1967)

69. R. J. W. Henry, P. G. Burke and A. L. Sinfailam, Phys. Rev. $\underline{178}$, 218 (1969)

70. S. Ormonde, K. Smith, B. W. Torres and A. R. Davies, Phy. Rev. A $\underline{8}$, 262 (1973)

71. K. A. Berrington, P. G. Burke and W. D. Robb, J. Phys. B: Atom. Mol. Phys. $\underline{8}$, 2500 (1975)

72. A. W. Ali, "Electron Impact Rate Coefficients for the Low Lying Metastable States of 0, 0^+, N and N^+", NRL Memo Report 3371 (1976)

73. E. J. Stone and E. C. Zipf, Phys. Rev. A $\underline{4}$, 610 (1971)

74. A. C. H. Smith, E. Caplinger, R. H. Neynaber, E. W. Rothe and S. M. Trujillo, Phys. Rev. $\underline{127}$, 1647 (1962)

75. S. J. Czyzak, T. K. Krueger, P. de A. P. Martins, H. E. Saraph and M. J. Seaton, Mon. Not. R. Astron. Soc. $\underline{148}$, 361 (1970)

76. H. E. Saraph, M. J. Seaton and J. Shemming, Proc. Phys. Soc. (London) $\underline{89}$, 27 (1966)

77. L. D. Thomas and R. K. Nesbet, Phys. Rev. A $\underline{11}$, 170 (1975)

78. Vo Ky Lan, N. Feautrier, M. Le Dourneuf and Van Regemorter, J. Phys. B $\underline{5}$, 1506 (1972)

79. S. P. Rountree and R. J. W. Henry, Phys. Rev. A $\underline{6}$, 2106 (1972)

80. T. Sawada and P. S. Ganas, Phys. Rev. A $\underline{7}$, 617 (1973)

81. W. L. Fite and R. T. Brackmann, Phys. Rev. $\underline{113}$, 815 (1959)

82. S. Trajmar, D. C. Cartwright and W. Williams, Phys. Rev. A $\underline{4}$, 1482 (1971)

83. P. S. Julienne and M. Krauss, J. of Res. , Nat. Bur. Stand. $\underline{76A}$, 661 (1972)

84. C. E. Watson, V. A. Dulock, Jr., R. S. Stolarski and A. E. S. Green, J. Geophy. Res. $\underline{72}$, 3961 (1967)

85. A. E. S. Green and R. S. Stolarski, J. Atm. Terr. Phys. $\underline{34}$, 1703 (1972)

86. A. Omholt, J. Atm. Terr. Phys. $\underline{10}$, 324 (1957)

87. M. McFarland, D. L. Albritton, F. C. Fehsenfeld, E. E. Ferguson and A. L. Schmeltekopf, J. Geophys. Res. $\underline{79}$, 2925 (1974)

88. M. McFarland, D. L. Albritton, F. C. Fehsenfeld, E. E. Ferguson and A. L. Schmeltekopf, J. Chem. Phys. $\underline{59}$, 6620 (1973)

89. T. Baurer and M. H. Bortner, Chapter 24, Defense Nuclear Agency Reaction Rate Handbook, 2nd Ed., Bortner and Baurer Eds., GE-TEMPO (1972)

90. F. C. Fehsenfeld, D. B. Dunkin and E. E. Ferguson, Planet. Space Sci. $\underline{18}$, 1267 (1970)

91. J. A. Rutherford and D. A. Vroom, J. Chem. Phys. $\underline{55}$, 5622 (1971)

92. R. F. Stebbings, B. R. Turner and J. A. Rutherford, J. Geophys. Res. $\underline{71}$, 771 (1966)

93. W. Lindinger, D. A. Albritton, F. C. Fehsenfeld and E. E. Ferguson, J. Geophys. Res. $\underline{80}$, 3725 (1975)

94. E. Graham IV, R. Johnsen and M. A. Biondi, J. Geophys. Res. $\underline{80}$, 2338 (1975)

95. M. McFarland, D. L. Albritton, F. C. Fehsenfeld, A. L. Schmeltekopf and E. E. Ferguson, J. Geophys. Res. $\underline{79}$, 2005 (1974)

96. R. H. Naynaber, J. A. Rutherford and D. A. Vroom, DNA Report 3384F, Defense Nuclear Agency (1974)

97. F. C. Fehsenfeld, Planet. Space Sci. $\underline{25}$, 195 (1977)

98. T. G. Slanger, B. J. Wood and G. J. Black, J. Geophys. Res. $\underline{76}$, 8430 (1971)

99. J. A. Meyer, D. W. Setser and D. H. Stedman, Astrophy. J. $\underline{157}$, 1023 (1969)

100. C. L. Lin and F. Kaufman, J. Chem. Phys. $\underline{55}$, 3760 (1971)

101. J. E. Davenport, T. G. Slanger and G. Black, J. Geophys. Res. $\underline{81}$, 12 (1976)

102. W. L. Fite and R. T. Brackmann, Proc. Sixth Int. Conf. Ioniz. Gases $\underline{1}$, p. 21, New York, North Holland Publishing Co. (1963)

103. D. Garvin, "Chemical Kinetics Data Survey IV", National Bureau of Standards NBSIR-73-203 (1973)

104. C. M. Lee, Phys. Rev. A $\underline{16}$, 109 (1977)

105. T. Baurer, General Electric, "Private Communication" (1977)

106. A. W. Ali, "Charge Exchange and Ion-Molecule Rearrangements in the Disturbed E and F Reactions" (Implications for Optical Emissions and Deionization)

107. L. Spitzer, Jr., "Physics of Fully Ionized Gases", Interscience Publishers, Inc., New York (1956)

108. E. R. Fisher and E. Bauer, J. Chem. Phys. 57, 1966 (1972)

109. G. R. Black, L. Sharpless and T. G. Slanger, J. Chem. Phys. 58, 4792 (1973), also T. Slanger and G. R. Black, J. Chem. Phys. 60, 468 (1974)

110. J. E. Morgan and H. I. Schiff, Can. J. Chem. 41, 903 (1963)

111. W. Felder and R. A. Young, J. Chem. Phys. 57, 572 (1972)

112. R. J. McNeal, M. E. Whitson, Jr. and G. R. Cook, J. Geophys. Res. 79, 1527 (1974)

113. W. D. Breshears and P. F. Bird, J. Chem. Phys. 48, 4768 (1968)

114. D. J. Eckstrom, J. Chem. Phys. 59, 2787 (1973)

DIRECTOR
Defense Advanced Rsch Proj Agency
Architect Building
1400 Wilson Blvd.
Arlington, Va. 22209
    ATTN: Strategic Tech Office

Defense Communication Engineer Center
1860 Wiehle Avenue
Reston, Va. 22090
    ATTN: CODE R820 R. L. Crawford
    ATTN: Code R410 W. D. Dehart

DIRECTOR
Defense Communications Agency
Washington, D. C. 20305
    ATTN: CODE 960
    ATTN: CODE 480

Defense Documentation Center
Cameron Station
Alexandria, Va. 22314   12 copies (if open publication)
    ATTN: TC   2 copies (if otherwise)

DIRECTOR
Defense Intelligence Agency
Washington, D. C. 20301
    ATTN: W. Wittig DC - 7D
    ATTN: DT-1B

DIRECTOR
Defense Nuclear Agency
Washington, D. C. 20305
    ATTN: STSI Archives
    ATTN: STVL
    ATTN: STTL Tech Library   2 copies
    ATTN: DDST
    ATTN: RAAE

DIR OF DEFENSE RSCH & ENGINEERING
Washington, D. C. 20301
    ATTN: DD/S&SS John B. Walsh
    ATTN: OAD/EPS

COMMANDER
Field Command
Defense Nuclear Agency
Kirtland AFB, NM 87115
    ATTN: FCPR
    ATTN   FCPR COL. John P. Hill
Interservice Nuclear Weapons School
Kirtland AFB, NM 87115
    ATTN: Document Control

DIRECTOR
Joint Strat TGT Planning Staff Jcs
Offutt AFB
Omaha, NB 68113
    ATTN: JLTW-2
    ATTN: JPST G. D. Burton
    ATTN: JPST MAJ. J. S. Green

CHIEF
Livermore Division Fld Command DNA
Lawrence Livermore Laboratory
P. O. Box 808
Livermore, CA 94550
    ATTN: FCPRL

COMMANDER
National Military Comd Sys Support Ctr
Pentagon
Washington, D. C. 20301
    ATTN: B211
    ATTN: DP DIRECTOR FOR CSPO

DIRECTOR
National Security Agency
Ft. George G. Meade, Md. 20755
    ATTN: W14 Pat Clark
    ATTN: Frank Leonard

OJCS/J-3
The Pentagon
Washington, D. C. 20301
ATTN: J-3 OPS ANAL BR. COL. Longsberry

OJCS/J-6
The Pentagon
Washington, D. C. 20301
    ATTN: J-6

DIRECTOR
Telecommunications & Comd & Con Sys
Washington, D. C. 20301
    ATTN: ASST DIR Info & Space Sys
    ATTN: DEP ASST. SEC Sys

Weapons Systems Evaluation Group
400 Army-Navy Drive
Arlington, Va. 22202
    ATTN: DOCUMENT CONTROL

COMMANDER
Harry Diamond Laboratories
2800 Powder Mill Road
Adelphi, Md. 20783
    ATTN: AMXDO-NP

COMMANDER
TRASANA
White Sands Missile Range, NM 88002
    ATTN: EAB

DIRECTOR
U. S. Army Ballistic Research Labs
Aberdeen Proving Ground, Md. 21003
    ATTN: AM-CA Franklin E. Niles

U. S. Army Communications CMD
C-B Services Division
Pentagon Rm. 2D513
Washington, D. C. 20310
   ATTN: CEAD

COMMANDER
U. S. Army Electronics Command
Fort Mommouth, N. J. 07703
    ATTN: AMSEL-TL-ENV Hans A. Bomke

COMMANDER
U. S. Army Material Command
5001 Eisenhower Avenue
Alexandria, Va. 22333
    ATTN: AMCRD-WN-RE John F. Corrigan

3

COMMANDER
U. S. Army Material Command
Foreign and Scientific Tech Center
220 7th St. N. E.
Charlottesville, Va. 22901
    ATTN: P. A. Crowley
    ATTN: R. Jones

COMMANDER
U. S. Army Missile Command
Redstone Arsenal
Huntsville, Al. 35809
    ATTN: AMSMI-YTT W. G. Preussel, Jr.

COMMANDER
U. S. Army Nuclear Agency
Fort Bliss, Tx. 79916
    ATTN: USANUA-W. J. Berbert
    ATTN: CDINS-E
CHIEF of Naval Research
Department of the Navy
Arlington, Ba. 22217
    ATTN: CODE 464 Jacob L. Warner
    ATTN: CODE 464 Thomas P. Quinn

COMMANDER
Naval Air Systems Command
Headquarters
Washington, D. C. 21360
    ATTN: AIR 5381

COMMANDER
Naval Electronics Systems Command
Naval Electronic System CMD HQS
Washington, D. C. 20360
    ATTN: NAVALEX 034 T. Barry Hughes
    ATTN: PME 106-1 Satellite Comm Project Off
    ATTN: John E. Doncarlos
    ATTN: PME 117

COMMANDER
Naval Electronics Laboratory Center
San Diego, CA 92152
    ATTN: William F. Moler
    ATTN: CODE 2200 Verne E. Hildebrand
    ATTN: R. Eastman

COMMANDING OFFICER
Naval Intelligence Support CTR
1301 Suitland Road, Bldg. 5
Washington, D.C. 20390
    ATTN: Mr. Dubbin Stic 12

COMMANDING OFFICER
Naval Research Laboratory
Washington, D.C. 20375
    ATTN: HDQ COMM DIR Bruce Wals
    ATTN: CODE 5460 Radio Propagation Br
    ATTN: CODE 6701 Jack D. Brown
    ATTN: 6700 Division Superintendent   25 copies (if unclassified)
                                                1 copy   (if classified)
    ATTN: CODE 6700.1 Dr. A. W. Ali   20 copies
    ATTN: CODE 6750 Branch Head
    ATTN: CODE 7127 Charles Y. Johnson

COMMANDING OFFICER
Naval Space Surveillance System
Dahlgren, VA 22448
    ATTN: Capt. J. H. Burton

COMMANDER
Naval Surface Weapons Center
White Oak, Silver Spring, MD 20910
    ATTN: CODE 1224 Navy Nuc Prgms Off
    ATTN: CODE 730 Tech. Lib.

DIRECTOR
Strategic Systems Project Office
Navy Department
Washington, D.C. 20376
    ATTN: NSP-2141

COMMANDER
ADC/AD
Ent AFB, CO. 80912
    ATTN: ADDA

Headquarters
U.S. Army Elect Warfare Lab (ECON)
White Sands Missile Range, NM 88002
    ATTN: E. Butterfield

AF Cambridge Rsch Labs, AFSC
L. G. Hanscom Field
Bedford, MA 01730
    ATTN: LKB Kenneth S. W. Champion
    ATTN: OPR James C. Ulwick
    ATTN: OPR Hervey P. Gauvin

5

AF Weapons Laboratory, AFSC
Kirtland AFB, NM 87117
    ATTN: John M. Kamm SAS
    ATTN: SUL
    ATTN: DYT LT Mark A. Fry
    ATTN: DYT CAPT Wittwer
    ATTN: DYT CAPT Gary Cable

AFTAC
Patrick AFB, Fl. 32925
    ATTN: TF MAJ. E. Hines
    ATTN: TF/CAPT. Wiley
    ATTN: TN

Air Force Avionics Laboratory, AFSC
Wright-Patterson AFB, Oh. 45433
    ATTN: AFAL AVWE Wade T. Hunt

Assistant Chief of Staff
Studies and Analysis
Headquarters, U. S. Air Force
Washington, D. C. 20330

Headquarters
Electronics Systems Division (AFSC)
L. G. Hanscom Field
Bedford, Ma. 01730
    ATTN: XRE LT. Michaels
    ATTN: LTC J. Morin CDEF XRC
    ATTN: YSEV

COMMANDER
Foreign Technology Division, AFSC
Wright-Patterson AFB, Oh. 45433
    ATTN: TD-BTA LIBRARY

HQ USAF/RD
Washington, D. C. 20330
    ATTN: RDQ

COMMANDER
Rome Air Development Center, AFSC
Griffith AFB, N. Y. 13440
    ATTN: EMTLD Doc Library

COMMANDER IN CHIEF
Strategic Air Command
Offutt AFB, NB 68113
    ATTN: XPFS MAJ. Brian G. Stephan

6

544IES
Offutt AFB, NB 68113
    ATTN: RDPO LT. Alan B. Merrill

Los Alamos Scientific Laboratory
P. O. Box 1663
Los Alamos, NM 87544
    ATTN: DOC CON for R. F. Taschek
    ATTN: DOC CON for Milton Peek
    ATTN: DOC CON for Eric Lindman
Sandia Laboratories
P. O. Box 5800
Albuquerque, NM 87115
    ATTN: DOC CON for A. Dean Thronbrough
    ATTN: DOC CON for W. D. Brown
    ATTN: DOC CON for D. A. Dahlgren, ORG 1722
    ATTN: DOC CON for J. P. Martin, ORG 1732
University of California
Lawrence Livermore Laboratory
P. O. Box 808
Livermore, CA 94550
    ATTN: Tech Info Dept L-3

Department of Commerce
National Oceanic & Atmospheric Admin.
Environmental Research Laboratories
Boulder, CO 80302
    ATTN: Joseph H. Pope
    ATTN: C. L. Rufenach

Department of Commerce
Office for Telecommunications
Institute for Telecom Science
Boulder, CO 80302
    ATTN: Glenn Falcon
    ATTN: G. Reed
    ATTN: L. A. Berry
    ATTN: William F. Utlaut

Department of Transportation
Transportation Rsch. System Center
Kendall Square
Cambridge, MA 02142
    ATTN: TER G. Harowles

NASA
Goddard Space Flight Center
Greenbelt, Md 20771
    ATTN: CODE 750 T. Golden

7

NASA
600 Independence Ave., S. W.
Washington, D. C. 20346
    ATTN: M. Dubin

Aerodyne Research, Inc.
Tech/Ops Building
20 South Avenue
Burlington, MA 01803
    ATTN: M. Camac
    ATTN: F. Bien

Aerospace Corporation
P. O. Box 92957
Los Angeles, CA 90009
    ATTN: T. M. Salmi
    ATTN: S. P. Bower
    ATTN: V. Josephson
    ATTN: SMFA for PWW
    ATTN: R. Grove
    ATTN: R. D. Rawcliffe
    ATTN: T. Taylor
    ATTN: Harris Mayer
    ATTN: D. C. Cartwright

Analytical Systems Corporation
25 Ray Avenue
Burlington, MA 01803
    ATTN: Radio Sciences

Avco-Everett Research Laboratory, Inc.
2385 Revere Beach Parkway
Everett, MA 02149
    ATTN: Richard M. Patrick

Boeing Company, The
P. O. Box 3707
Seattle, WA 98124
    ATTN: D. Murray
    ATTN: Glen Keister

Brown Engineering Company, Inc.
Cummings Research Park
Huntsville, AL 35807
    ATTN: David Lambert MS 18

California at San Diego, Univ. of
Building 500 Mather Campus
3172 Miramar Road
La Jolla, CA 92037
    ATTN: Henry G. Booker

Calspan
P. O. Box 235
Buffalo, N. Y. 14221
    ATTN: Romeo A. Deliberis

Computer Sciences Corporation
P. O. Box 530
6565 Arlington Blvd.
Falls Church, VA 22046
    ATTN: H. Blank
    ATTN: Barbara F. Adams

Comsat Laboratories
P. O. Box 115
Clarksburg, Md. 20734
    ATTN: R. R. Taur

Cornell University
Department of Electrical Engineering
Ithaca, N. Y. 14850
    ATTN: D. T. Farley, Jr.

ESL, Inc.
495 Java Drive
Sunnyvale, CA 93102
    ATTN: J. Roberts
    ATTN: V. L. Mower
    ATTN: James Marshall
    ATTN: R. K. Stevens

General Electric Company
Tempo-Center for Advanced Studies
816 State Street
Santa Barbara, CA 93102
    ATTN: Don Chandler
    ATTN: DASIAC
    ATTN: Tim Stephens

General Electric Company
P. O. Box 1122
Syracuse, N. Y. 13201
    ATTN: F. A. Reibert

General Research Corporation
P. O. Box 3587
Santa Barbara, CA 93105
    ATTN: John Ise, Jr.

9

Geophysical Institute
University of Alaska
Fairbanks, AK 99701
    ATTN: Technical Library
    ATTN: Neil Brown
    ATTN: T. N. Davis

GTE Sylvania, Inc.
189 B Street
Needham Heights, MA 02194
    ATTN: Marshall Cross

HRB-SINGER, Inc.
Science Park, Science Park Road
P. O. Box 60
State College, PA 16801
    ATTN: Larry Feathers

Honeywell Incorporated
Radiation Center
2 Forbes Road
Lexington, MA   02173
    ATTN: W. Williamson

Illinois, University of
Department of Electrical Engineering
Urbana, IL 61801
    ATTN: K. C. Yeh

Institute for Defense Analyses
400 Army-Navy Drive
Arlington, VA 22202
    ATTN: Ernest Bauer
    ATTN: Hans Wolfhard
    ATTN: J. M. Aein
    ATTN: Joel Bengston

Intl Tel & Telegraph Corporation
500 Washington Avenue
Nutley, N. J. 07110
    ATTN: Technical Library

ITT Electro-Physics Laboratories, Inc.
9140 Old Annapolis Road
Columbus, Md. 21043
    ATTN: John M. Kelso

Johns Hopkins University
Applied Physics Laboratory
8621 Georgia Avenue
Silver Spring, MD 20910
    ATTN: Document Librarian

Lockheed Missiles & Space Co., Inc.
P. O. Box 504
Sunnyvale, CA 94088
    ATTN: Dept. 60-12

Lockheed Missiles and Space Company
3251 Hanover Street
Palo Alto, CA 94304
    ATTN: Billy M. McCormac, Dept 52-14
    ATTN: Martin Walt, Dept 52-10
    ATTN: Richard G. Johnson, Dept 52-12
    ATTN: JOHN CLADIS

MIT Lincoln Laboratory
P. O. Box 73
Lexington, MA 02173
    ATTN: Mr. Walden, X113
    ATTN: D. Clark
    ATTN: James H. Pannell, L-246
    ATTN: Lib A-082 for David M. Towle

Martin Marietta Corporation
Denver Distribution
P. O. Box 179
Denver, CO 80201
    ATTN: Special Projects Program 248

Maxwell Laboratories, Inc.
9244 Balboa Avenue
San Diego, CA 92123
    ATTN: A. J. Shannon
    ATTN: V. Fargo
    ATTN: A. N. Rostocker

McDonnell Douglas Corporation
5301 Bolsa Avenue
Huntington Beach, CA 92657
    ATTN: J. Moule
    ATTN: N. Harris

Mission Research Corporation
735 State Street
Santa Barbara, CA   93101
    ATTN: R. Hendrick
    ATTN: Conrad L. Longmire
    ATTN: Ralph Kilb
    ATTN: R. E. Rosenthal
    ATTN: R. Bogusch
    ATTN: David Sowle
    ATTN: M. Scheibe
    ATTN: P. Fischer
Mitre Corporation, The
Route 62 and Middlesex Turnpike
P. O. Box 208
Bedford, MA   01730
    ATTN: Chief Scientist W. Sen
    ATTN: S. A. Morin M/S
    ATTN: C. Harding

North Carolina State Univ At Raleigh
Raleigh, N. C.   27507
    ATTN: SEC Officer for Walter A. Flood

Pacific-Sierra Research Corp.
1456 Cloverfield Blvd.
Santa Monica, CA   90404
    ATTN: E. C. Field, Jr.

Philco-Ford Corporation
Western Development Laboratories Div
3939 Fabian Way
Palo Alto, CA   94303
    ATTN: J. T. Mattingley MS X22

Photometrics, Inc.
442 Marrett Road
Lexington, MA   02173
    ATTN: Irving J. Kofsky

Mitre Corporation, The
Westgate Research Park
1820 Dolley Madison Blvd.
McLean, VA   22101
    ATTN: Allen Schneider

Physical Dynamics, Inc.
P. O. Box 1069
Berkeley, CA 94701
    ATTN: Joseph B. Workman

Physical Sciences, Inc.
607 North Avenue, Door 18
Wakefield, MA 01880
    ATTN: Kurt Wray

R & D Associates
P. O. Box 3580
Santa Monica, CA 90403
    ATTN: Robert E. Lelevier
    ATTN: Forest Gilmore
    ATTN: Richard Latter
    ATTN: William B. Wright, Jr.

R & D Associates
1815 N. Ft. Myer Drive
11th Floor
Arlington, VA 2209
    ATTN: Herbert J. Mitchell

Rand Corporation, The
1700 Main Street
Santa Monica, CA 90406
    ATTN: Cullen Crain

Science Applications, Inc.
P. O. Box 2351
La Jolla, CA 92038
    ATTN: Daniel A. Hamlin
    ATTN: D. Sachs
    ATTN: E. A. Straker

Space Data Corporation
1331 South 26th Street
Phoenix, AZ 85034
    ATTN: Edward F. Allen

Stanford Research Institute
333 Ravenswood Avenue
Menlo Park, CA 94025
ATTN: M. Baron
ATTN: L. L. Cobb
ATTN: Walter G. Chestnut
ATTN: David A. Johnson
ATTN: Charles L. Rino
ATTN: E. J. Fremouw
ATTN: Ray L. Leadabrand
ATTN: Donald Neilson

Stanford Research Institute
306 Wynn Drive, N. W.
Huntsville, AL 35805
ATTN: Dale H. Davis

Technology International Corporation
75 Wiggins Avenue
Bedford, MA 01730
ATTN: W. P. Boquist

TRW Systems Group
One Space Park
Redondo Beach, CA 90278
ATTN: P. H. Katsos
ATTN: J. W. Lowery

Utah State University
Logan, UT 84321
ATTN: C. Wyatt
ATTN: D. Burt
ATTN: Kay Baker
ATTN: Doran Baker

Visidyne, Inc.
19 Third Avenue
North West Industrial Park
Burlington, MA 01803
ATTN: William Reidy
ATTN: Oscar Manley
ATTN: J. W. Carpenter

14